

Alternating minimization algorithms for graph regularized tensor completion

Yu Guan*, Shuyu Dong*, P.-A. Absil* and François Glineur†

†ICTEAM and †CORE, UCLouvain, Louvain-la-Neuve, Belgium.

Abstract. We consider a low-rank tensor completion (LRTC) problem which aims to recover a tensor from incomplete observations. LRTC plays an important role in many applications such as signal processing, computer vision, machine learning, and neuroscience. A widely used approach is to combine the tensor completion data fitting term with a regularizer based on a convex relaxation of the multilinear ranks of the tensor. For the data fitting function, we model the tensor variable by using the Canonical Polyadic (CP) decomposition and for the low-rank promoting regularization function, we consider a graph Laplacian-based function which exploits correlations between the rows of the matrix unfoldings. For solving our LRTC model, we propose an efficient alternating minimization algorithm. Furthermore, based on the Kurdyka-Łojasiewicz property, we show that the sequence generated by the proposed algorithm globally converges to a critical point of the objective function. Besides, an alternating direction method of multipliers algorithm is also developed for the LRTC model. Extensive numerical experiments on synthetic and real data indicate that the proposed algorithms are effective and efficient.

Key words. Kurdyka-Łojasiewicz property, tensor completion, conjugate gradient, alternating direction method of multiplier, alternating minimization

AMS subject classifications. 15A69, 49M20, 65B05, 90C26, 90C30, 90C52

1. Introduction. In the literature on low-rank matrix completion, the matrix nuclear norm is proven [12, 51] to be a convex relaxation of the matrix rank that guarantees exact solutions to the corresponding rank-constrained problem in some specific circumstances and has been used in various matrix rank-constrained problems [42] such as matrix completion. Generalized from this matrix relaxation, several works [24, 40, 53, 60] extended the nuclear norm-based regularization to the completion of partially observed tensors (also known as multidimensional arrays). Liu et al. [39] first introduced an extension of nuclear norm to the low-rank tensor completion (LRTC) problem and later defined the nuclear norm of a tensor as a convex combination of nuclear norms of its unfolding matrices in [40]. For a given tensor $\mathcal{T} \in \mathbb{R}^{m_1 \times \dots \times m_k}$, its low-rank tensor completion model is as follows,

$$(1.1) \quad \min_{\mathcal{Z} \in \mathbb{R}^{m_1 \times \dots \times m_k}} \frac{1}{2} \|\mathcal{P}_\Omega(\mathcal{T} - \mathcal{Z})\|_F^2 + \sum_{i=1}^k \lambda_i \|\mathcal{Z}_{(i)}\|_*,$$

where \mathcal{P}_Ω is the projection operator that only retains the *revealed* entries of \mathcal{T} , recorded in the index set $\Omega \subset \llbracket m_1 \rrbracket \times \dots \times \llbracket m_k \rrbracket$, and $\|\mathcal{Z}_{(i)}\|_*$ denotes the matrix *nuclear norm* of the mode- i matricization (Definition 2.3) of tensor \mathcal{Z} . The penalty terms $\|\mathcal{Z}_{(i)}\|_*$ in (1.1) promote solutions such that the matricizations of the tensor variable \mathcal{Z} have a low rank.

However, model (1.1) suffers from high computational cost as it needs to solve a singular value decomposition of very large unfolding matrices at each iteration. Therefore, some LRTC models are

*Email: ricky7guanyu@gmail.com, {shuyu.dong,pa.absil,francois.glineur}@uclouvain.be. This work was supported by the Fonds de la Recherche Scientifique – FNRS and the Fonds Wetenschappelijk Onderzoek – Vlaanderen under EOS Project no. 30468160. The second author is supported by the FNRS through a FRIA scholarship.

based on low-rank tensor decomposition, see [3, 16, 31, 45, 56]. Two popular decompositions of high order tensors are the Tucker decomposition [19, 20, 30, 57] and the Canonical Polyadic (CP) decomposition [13, 22, 28, 33]. In this paper, we focus on the CP approach which has been applied to the LRTC problem in [1, 10, 11, 32, 35, 56]. Other decomposition approaches applying to the LRTC problem are hierarchical tensor representations [18, 49, 50] and PARAFAC2 models [49].

On the other hand, inter-relations between data entries, through auxiliary information for example, have recently been exploited to improve the completion accuracy for the LRTC task. This idea is motivated from [48] whose model includes the graph Laplacian for matrix completion as follows

$$(1.2) \quad \min_{W, H} \frac{1}{2} \|\mathcal{P}_\Omega(Y - WH^\top)\|_F^2 + \frac{1}{2} \langle WW^\top, L_w \rangle + \frac{1}{2} \langle HH^\top, L_h \rangle,$$

where L_w and L_h are the shifted graph Laplacian which will be introduced in detail in Section 3. In a similar way, graph Laplacian-based regularization has also been applied to LRTC problems, see [44, 25, 26]. Other approaches with a probabilistic perspective can be found in [6, 36, 61, 62].

The main contributions of this paper are as follows.

- In this paper, we build our LRTC model based on the nuclear norm approach, CP decomposition approach and graph Laplacian regularizer. To our knowledge, this is a new LRTC model and will be shown to be an useful regularized model that ensures improvements in the recovery accuracy over graph-agnostic models, especially when the fraction of revealed data is small; see Section 6.1.
- We provide an alternating minimization algorithm for solving the graph-regularized tensor completion problem. An efficient Hessian-vector multiplication scheme is used in the linear conjugate gradient (CG) algorithm for solving the subproblems in this alternating minimization framework. The computational framework of the linear CG algorithm is inspired by Rao et al. [48] for graph-regularized matrix completion. In addition, an alternating direction method of multipliers (ADMM) algorithm is also proposed; see Section 4.1.
- We provide a proof for the convergence of iterates of the proposed AltMin algorithm to a critical point of the objective function according to the Kurdyka-Łojasiewicz (KŁ) property; see Section 5.
- We show through experiments (Section 6) on both synthetic and real data that our algorithms produce tensor completion results with good recovery accuracies and are time efficient compared to several baseline methods.

We organize this paper as follows. We begin with the introduction of some notations in Section 2. In Section 3, our LRTC model with a graph Laplacian-based regularizer is introduced. In Section 4, an alternating minimization (AltMin) algorithm using linear CG for solving the subproblems is proposed; an ADMM algorithm is also developed for solving the graph-regularized LRTC problem. Convergence analysis of the AltMin algorithm is given in Section 5. Numerical experiments together with some interesting observations are presented in Section 6. Conclusion is shown in Section 7.

2. Terminology. In this section, we introduce the definition and notation of some tensor operations. A real-valued order- k tensor is defined as $\mathcal{Z} = [z_{\ell_1, \dots, \ell_k}] \in \mathbb{R}^{m_1 \times m_2 \times \dots \times m_k}$, where an element $z_{\ell_1, \dots, \ell_k}$ is accessed via k indices (ℓ_1, \dots, ℓ_k) . The index set $\{1, \dots, m\}$ is denoted by $\llbracket m \rrbracket$.

Definition 2.1 (Kronecker Product). The Kronecker product of vectors $\mathbf{u} = [u_\ell] \in \mathbb{R}^{m_1}$ and $\mathbf{v} = [v_\ell] \in \mathbb{R}^{m_2}$ results in a vector $\mathbf{u} \otimes \mathbf{v} \in \mathbb{R}^{m_1 m_2}$ defined as

$$(2.1) \quad \mathbf{u} \otimes \mathbf{v} = [u_1 \mathbf{v}^\top, u_2 \mathbf{v}^\top \cdots u_{m_1} \mathbf{v}^\top]^\top.$$

More compactly, we have $(\mathbf{u} \otimes \mathbf{v})_{m_2(\ell_1-1)+\ell_2} = u_{\ell_1} v_{\ell_2}$ for $\ell_1 \in \llbracket m_1 \rrbracket$ and $\ell_2 \in \llbracket m_2 \rrbracket$.

Definition 2.2 (Khatri-Rao Product). The Khatri-Rao product $U \odot V$ of two matrices $U = [u_{\ell,r}] \in \mathbb{R}^{m_1 \times R}$ and $V = [v_{\ell,r}] \in \mathbb{R}^{m_2 \times R}$ with the same column number is a matrix of size $m_1 m_2 \times R$ whose r -th column is $u_{:,r} \otimes v_{:,r}$.

Definition 2.3 (Tensor matricization). The mode- i matricization $\mathcal{Z}_{(i)}$ is the unfolding of a tensor $\mathcal{Z} \in \mathbb{R}^{m_1 \times m_2 \times \cdots \times m_k}$ along its i -th mode of size $m_i \times (\prod_{j \neq i} m_j)$. The tensor element $z_{\ell_1, \dots, \ell_k}$ in \mathcal{Z} is identified with the matrix element $[\mathcal{Z}_{(i)}]_{\ell_i, r_i}$ in $\mathcal{Z}_{(i)}$, where

$$(2.2) \quad r_i = 1 + \sum_{\substack{n=1 \\ n \neq i}}^k (\ell_n - 1) I_n, \quad \text{with,} \quad I_n = \prod_{\substack{j=1 \\ j \neq i}}^{n-1} m_j$$

Definition 2.4 (CP Decomposition). The Canonical Polyadic (CP) decomposition [13, 22, 28, 30, 33] of a tensor $\mathcal{Z} \in \mathbb{R}^{m_1 \times \cdots \times m_k}$ is defined as

$$(2.3) \quad \mathcal{Z} = \llbracket U^{(1)}, \dots, U^{(k)} \rrbracket = \sum_{r=1}^R u_{:,r}^{(1)} \circ \dots \circ u_{:,r}^{(k)},$$

where $U^{(i)} = [u_{\ell,r}^{(i)}] \in \mathbb{R}^{m_i \times R}$ for $i = 1, \dots, k$ and \circ denotes the outer product. An equivalent CP form can be written as

$$(2.4) \quad \mathcal{Z}_{(i)} = U^{(i)} (U^{(k)} \odot \dots \odot U^{(i+1)} \odot U^{(i-1)} \odot \dots \odot U^{(1)})^\top = U^{(i)} [(U^{(j)})^{\odot_{j \neq i}}]^\top,$$

where $\mathcal{Z}_{(i)}$ is the mode- i tensor matricization.

Definition 2.5 (Tensor Inner Product). The inner product of two tensors $\mathcal{Z}^{(1)}, \mathcal{Z}^{(2)} \in \mathbb{R}^{m_1 \times m_2 \times \cdots \times m_k}$ of the same size is defined as follows

$$(2.5) \quad \langle \mathcal{Z}^{(1)}, \mathcal{Z}^{(2)} \rangle = \sum_{\ell_1=1}^{m_1} \cdots \sum_{\ell_k=1}^{m_k} z_{\ell_1 \dots \ell_k}^{(1)} z_{\ell_1 \dots \ell_k}^{(2)}.$$

Definition 2.6 (Tensor Frobenius Norm). Generalized from matrix Frobenius norm, the Frobenius of a tensor $\mathcal{Z} \in \mathbb{R}^{m_1 \times m_2 \times \cdots \times m_k}$ is defined as

$$\|\mathcal{Z}\|_F = \sqrt{\langle \mathcal{Z}, \mathcal{Z} \rangle} = \sqrt{\sum_{\ell_1=1}^{m_1} \cdots \sum_{\ell_k=1}^{m_k} z_{\ell_1 \dots \ell_k}^2}.$$

To conclude this section, the following lemma shows the relation between the nuclear norm of a matrix and the Frobenius norm of its decomposed matrices.

Lemma 2.7. [23, 54, 55, Lemma 1] The nuclear norm of a matrix $X \in \mathbb{R}^{m_1 \times m_2}$ can be defined as

$$(2.6) \quad \|X\|_* := \min_{U, V: UV^\top = X} \frac{1}{2} \{ \|U\|_F^2 + \|V\|_F^2 \}.$$

3. Problem setting. In this section, we introduce our LRTC model in the form of CP decomposition with a graph Laplacian-based regularization,

$$(3.1) \quad \min_{U^{(1)}, \dots, U^{(k)}} \frac{1}{2} \|\mathcal{P}_\Omega(\mathcal{T} - \llbracket U^{(1)}, \dots, U^{(k)} \rrbracket)\|_F^2 + \sum_{i=1}^k \frac{\lambda_i}{2} \langle U^{(i)} U^{(i)\top}, L^{(i)} \rangle + \sum_{i=1}^k \frac{\lambda_i}{2} \|(U^{(j)})^{\odot_{j \neq i}}\|_F^2,$$

where $\Omega \subset \llbracket m_1 \rrbracket \times \dots \times \llbracket m_k \rrbracket$ is the index set of the revealed entries and \mathcal{T} is the ground truth tensor that is known only on Ω . The proportion of the known entries $|\Omega|/(m_1 \dots m_k)$, or its expectation $\mathbb{E}[|\Omega|]/(m_1 \dots m_k)$, is referred to as the sampling rate ρ . The shifted graph Laplacian $L^{(i)}$ is defined as

$$(3.2) \quad L^{(i)} = \lambda_L \mathbf{Lap}^{(i)} + I_{m_i},$$

where $\mathbf{Lap}^{(i)}$ is the graph Laplacian matrix which is assumed to be known. The parameters $\lambda_i \geq 0$ and $\lambda_L \geq 0$ control the trade-off between the training error function and the regularization term. In particular, when $\lambda_L = 0$, problem (3.1) reduces to a graph-agnostic tensor completion model. The search space of (3.1) is $\mathbb{R}^{m_1 \times R} \times \dots \times \mathbb{R}^{m_k \times R}$.

Throughout this paper, the graph Laplacian matrices involved in the regularization term are defined as follows. For an undirected graph, denoted as $\mathcal{G} := (\mathcal{V}, \mathcal{E})$, let $W \in \mathbb{R}^{|\mathcal{V}| \times |\mathcal{V}|}$ denote a weighted graph adjacency matrix of \mathcal{G} . The Laplacian matrix is denoted and defined as

$$(3.3) \quad \mathbf{Lap} = \text{diag}(W\mathbf{1}) - W.$$

Based on calculations in [17, Section 1.4], a Laplacian matrix $\mathbf{Lap} \in \mathbb{R}^{m \times m}$ defined as in (3.3) has the following property for any $F \in \mathbb{R}^{m \times R}$,

$$(3.4) \quad \langle FF^\top, \mathbf{Lap} \rangle = \sum_{\ell_1=1}^m \sum_{\ell_2=1}^m W_{\ell_1 \ell_2} \|F_{\ell_1, :} - F_{\ell_2, :}\|_2^2.$$

The regularization term of (3.1) is an extension of the graph Laplacian-based regularization [48] to tensor completion and is related to a generalized nuclear norm of the matricizations $\mathcal{Z}_{(i)}$ of the tensor variable. Note that the standard nuclear norm of a matricization of \mathcal{Z} satisfies the following characterization,

$$(3.5) \quad \|\mathcal{Z}_{(i)}\|_* = \min_{U^{(i)} [(U^{(j)})^{\odot_{j \neq i}}]^\top = \mathcal{Z}_{(i)}} \frac{1}{2} \{ \|U^{(i)}\|_F^2 + \|(U^{(j)})^{\odot_{j \neq i}}\|_F^2 \}.$$

It has been observed that combining graph-based information with a LRTC model enhances the completion accuracy especially when the observed entries are sparse; see [25, 26, 44]. Note that when $k = 2$, the problem reduces to a matrix completion problem and the model is equivalent to the graph-regularized model (1.2).

4. Algorithms. In this section, we introduce an alternating minimization (AltMin) algorithm and an ADMM algorithm for solving the LRTC problem (3.1).

4.1. Alternating minimization. To minimize the objective function of (3.1), defined on the product space of tensor factors $\mathbb{R}^{m_1 \times R} \times \dots \times \mathbb{R}^{m_k \times R}$, alternating minimization (also referred to as block coordinate descent) consists in minimizing the function cyclically over each factor matrix among $(U^{(1)}, \dots, U^{(k)})$ while keeping the remaining variables fixed at their last updated values.

Let $f(\cdot)$ denote the objective function of (3.1) and $U_t^{(i)}$ denote the t -th iterate of $U^{(i)}$ for $t \geq 0$. Let $f_{t+1}^{(i)}$ denote the objective function of the subproblem in $U^{(i)}$ as follows:

$$(4.1) \quad f_{t+1}^{(i)}(U^{(i)}) \triangleq f(U_{t+1}^{(1)}, \dots, U_{t+1}^{(i-1)}, U^{(i)}, U_t^{(i+1)}, \dots, U_t^{(k)}).$$

Algorithm 4.1 Alternating minimization

Input: Data (known on Ω) $\mathcal{P}_\Omega(\mathcal{T}) \in \mathbb{R}^{m_1 \times \dots \times m_k}$, observed set Ω . Objective function f

Output: $(U_t^{(i)})_{i=1, \dots, k}$

- 1: Initialization: $U_0^{(1)}, \dots, U_0^{(k)}$
 - 2: **for** $t = 0, 1, 2, \dots$ **do**
 - 3: **if** stopping criterion is satisfied **then**
 - 4: return;
 - 5: **end if**
 - 6: **for** $i = 1, \dots, k$ **do**
 - 7: $U_{t+1}^{(i)} = \arg \min_{U \in \mathbb{R}^{m_i \times R}} f_{t+1}^{(i)}(U)$
 - 8: **end for**
 - 9: **end for**
-

During the $(t+1)$ -th iteration and for $i \in \llbracket k \rrbracket$, subproblem (4.1) has the following expression¹:

$$(4.2) \quad \min_{U^{(i)} \in \mathbb{R}^{m_i \times R}} \frac{1}{2} \|\mathcal{P}_{\Omega^{(i)}}(\mathcal{T}_{(i)} - U^{(i)}[(U^{(j)})^{\odot_{j \neq i}}]^\top)\|_F^2 + \frac{\lambda_i}{2} \langle U^{(i)} U^{(i)\top}, L^{(i)} \rangle + \sum_{\substack{j=1 \\ j \neq i}}^k \frac{\lambda_j}{2} \|(U^{(j)})^{\odot_{n \neq j}}\|_F^2,$$

where $\Omega^{(i)}$ is the set of 2-dimensional indices, in the form of $(\ell_i, r_i) \in \Omega^{(i)}$, corresponding to $(\ell_1, \dots, \ell_k) \in \Omega$ with respect to the tensor matricization (Definition 2.3). The one-to-one map satisfies (2.2).

Due to the graph Laplacian-based regularization term, the major challenge in solving (3.1) by the alternating minimization procedure is the structure of each subproblem, which is different from those of an unregularized tensor decomposition problem. We explain this in detail as follows. For clarity and practical reasons, we show this by first converting the matrix variable $U^{(i)}$ into its vectorization $\mathbf{x} := \text{vec}(U^{(i)\top}) \in \mathbb{R}^{m_i R}$ and then studying $g^{(i)}(\mathbf{x}) := f_{t+1}^{(i)}(U^{(i)})$. The function g is a quadratic function of the following form,

$$(4.3) \quad g^{(i)}(\mathbf{x}) := \frac{1}{2} \mathbf{x}^\top M^{(i)} \mathbf{x} - \text{vec}(Q^{(i)})^\top \mathbf{x}, \quad \mathbf{x} \in \mathbb{R}^{m_i R},$$

¹For convenience, we ignore the subscript $t+1$ or t in the variables $U^{(j)}$ for all $j = 1, \dots, k$, and omit constant terms in the objective.

where

$$M^{(i)} = A^{(i)} + \lambda_i L^{(i)} \otimes I_R + I_{m_i} \otimes C^{(i)} \in \mathbb{R}^{m_i R \times m_i R}, \quad (4.4a)$$

$$Q^{(i)} = (\mathcal{P}_{\Omega^{(i)}} \mathcal{T}_{(i)})(U^{(j)})^{\odot_{j \neq i}} \in \mathbb{R}^{m_i \times R}. \quad (4.4b)$$

The components $A^{(i)}$ and $C^{(i)}$ in (4.4a) are defined and computed as follows: Let $A^{(i)} \in \mathbb{R}^{m_i R \times m_i R}$ be the matrix of the following quadratic form $\mathbf{x}^T A^{(i)} \mathbf{x} := \|\mathcal{P}_{\Omega^{(i)}}(U^{(i)}[(U^{(j)})^{\odot_{j \neq i}}]^\top)\|_F^2$ in $\mathbf{x} := \text{vec}(U^{(i)})$. We have

$$(4.5) \quad \begin{aligned} \frac{1}{2} \|\mathcal{P}_{\Omega^{(i)}}(U^{(i)}[(U^{(j)})^{\odot_{j \neq i}}]^\top)\|_F^2 &= \frac{1}{2} \langle U^{(i)} U^{(-i)T}, P_{\Omega^{(i)}}(U^{(i)} U^{(-i)T}) \rangle \\ &= \frac{1}{2} \text{Tr}(U^{(-i)} U^{(i)T} P_{\Omega^{(i)}}(U^{(i)} U^{(-i)T})) = \frac{1}{2} \sum_{s=1}^{m_i} U^{(-i)} U_{s,:}^T P_{\Omega_s^{(i)}}(U_{s,:} U^{(-i)T}) \end{aligned}$$

$$(4.6) \quad = \frac{1}{2} \sum_{s=1}^{m_i} U_{s,:} U^{(-i)T} P_{\Omega_s^{(i)}}(U^{(-i)} U_{s,:}^T) = \frac{1}{2} \sum_{s=1}^{m_i} U_{s,:} \sum_{\ell \in \Omega_s^{(i)}} (d_{\ell,:}^{(i)})^\top d_{\ell,:}^{(i)} U_{s,:}^\top,$$

where $U_{s,:}$ denotes the s -th row of $U^{(i)}$, $U^{(-i)}$ denotes $(U^{(j)})^{\odot_{j \neq i}} \in \mathbb{R}^{m_{(-i)} \times R}$ and $m_{(-i)}$ denotes the number $\prod_{j \neq i} m_j$ for brevity. The equation (4.6) holds under the following convention: the projection $P_{\Omega_s^{(i)}}$ (defined on $\mathbb{R}^{m_{(-i)}}$ by default) applies to each of the columns of $U^{(-i)}$, which has the effect of projecting any row of $U^{(-i)}$ with index $\ell \notin \Omega_s^{(i)}$ to a row of zeros. Therefore, $A^{(i)} \in \mathbb{R}^{m_i R \times m_i R}$ is a block diagonal matrix with m_i diagonal blocks and each block has the form

$$(4.7) \quad A_s^{(i)} = \sum_{\ell \in \Omega_s^{(i)}} (d_{\ell,:}^{(i)})^\top d_{\ell,:}^{(i)},$$

where $\Omega_s^{(i)} = \{\ell : (s, \ell) \in \Omega^{(i)}\}$ and $d_{\ell,:}$ is the ℓ -th row of $(U^{(j)})^{\odot_{j \neq i}}$.

The component $I_{m_i} \otimes C^{(i)}$ denotes the matrix related to the quadratic form

$$(4.8) \quad q(U^{(i)}) := \sum_{j \neq i} \lambda_j \|(U^{(n)})^{\odot_{n \neq j}}\|_F^2$$

in (4.2). Now we verify that

$$(4.9) \quad C^{(i)} = \sum_{\substack{j=1 \\ j \neq i}}^k \lambda_j \text{diag}[(\|U_{:, \ell}^{(-i, -j)}\|^2)_{\ell=1, \dots, R}] \in \mathbb{R}^{R \times R},$$

where $U^{(-i, -j)} := (U^{(n)})^{\odot_{n \neq i, j}}$ denotes the Khatri-Rao product of $U^{(n)}$'s excluding $U^{(i)}$ and $U^{(j)}$. Indeed, the function (4.8) writes

$$(4.10) \quad \begin{aligned} q(U^{(i)}) &= \sum_{j \neq i} \lambda_j \sum_{\ell=1}^R \|U_{:, \ell}^{(-i, -j)} \otimes U_{:, \ell}^{(i)}\|_2^2 = \sum_{j \neq i} \lambda_j \sum_{\ell=1}^R \underbrace{\|U_{:, \ell}^{(-i, -j)}\|_2^2}_{C_{\ell \ell}^{(i, j)}} \text{Tr}(U_{:, \ell}^{(i)} U_{:, \ell}^{(i)T}) \\ &= \sum_{j \neq i} \lambda_j \text{Tr}(U^{(i)} C^{(i, j)} U^{(i)T}) = \text{Tr}[U^{(i)} (\sum_{j \neq i} \lambda_j C^{(i, j)}) U^{(i)T}]. \end{aligned}$$

By recalling that $\text{Tr}(X^T C X) = \text{vec}(X)^T (I \otimes C) \text{vec}(X)$, the formula (4.9) of $C^{(i)}$ yields the identification $q(U^{(i)}) = \mathbf{x}^T (I_{m_i} \otimes C^{(i)}) \mathbf{x}$, with $\mathbf{x} = \text{vec}(U^{(i)T})$.

The function $g^{(i)}$ in (4.3), and equivalently $f_{t+1}^{(i)}$ of (4.2), is strongly convex (see Theorem 5.7 point 2) provided that $\lambda_n > 0$ for $n = 1, \dots, k$. As a consequence, the update step (4.2) consists of finding the graph-regularized least squares solution

$$(4.11) \quad M^{(i)} \mathbf{x}^* = \text{vec}(Q^{(i)}).$$

Note that the main computational challenge in finding the least-squares solution (4.11) is the presence of graph Laplacian-based regularization terms in (4.3). The similar difficulty can be found in the graph-regularized least squares problem in [48]. More precisely, the matrix $M^{(i)} \in \mathbb{R}^{m_i R \times m_i R}$ in (4.3) is not block diagonal because of the component $L^{(i)} \otimes I_R$. Therefore, the least squares problem with (4.3) cannot be decomposed into m_i separable least squares problems in \mathbb{R}^R . In the next subsection, we use linear CG to solve each subproblem with respect to its vectorized form. We also consider (in Section 4.3) an alternating direction method of multipliers (ADMM) as an alternative way to address the difficulty with these nonseparable least squares problems.

The stopping criterion in Algorithm 4.1 (line 3) is satisfied if either of the following conditions is satisfied: (i) the wall time used for producing the latest iterate is larger than a time budget parameter τ_{\max} (which is potentially set to ∞); (ii) the progress of the iterate $(U_t^{(i)})_{i=1, \dots, k}$, measured by a heuristic difference function Δ_t , is smaller than a (global) tolerance parameter ϵ . Here we define Δ_t as follows,

$$(4.12) \quad \Delta_t := |E(U_t; \Omega_{\text{tr}}) - E(U_{t-1}; \Omega_{\text{tr}})|,$$

where $E(U; \Omega_{\text{tr}}) := \frac{\|P_{\Omega_{\text{tr}}}(\llbracket U^{(1)}, \dots, U^{(k)} \rrbracket - \mathcal{T})\|_F}{\|P_{\Omega_{\text{tr}}}(\mathcal{T})\|_F}$ is the relative error restricted to the index set $\Omega_{\text{tr}} \subset \llbracket m_1 \rrbracket \times \dots \times \llbracket m_k \rrbracket$ of the revealed entries.²

In the following subsections, we consider linear CG for solving the high-dimensional least-squares problem (4.3).

4.2. The linear CG solver. Algorithm 4.2 shows an instance of AltMin using linear CG as the subproblem solver. Detailed steps for the linear CG algorithm are given in Algorithm 4.3.

Note that $M^{(i)}$ has a special form which contains Kronecker products and its size is very large, hence we compute it in a more efficient way by a special Hessian-vector multiplication in the CG method. By the relation $(B^T \otimes A) \text{vec}(X) = \text{vec}(A X B)$, it follows that

$$\begin{aligned} (L^{(i)} \otimes I_R) \mathbf{x} &= \text{vec}(U^{(i)T} L^{(i)}), \\ (I_{m_i} \otimes C^{(i)}) \mathbf{x} &= \text{vec}(C^{(i)} U^{(i)T}), \end{aligned}$$

where $\mathbf{x} = \text{vec}(U^{(i)T})$. Thus the Hessian-vector multiplication can be implemented by a series of matrix multiplications as follows

$$(4.13) \quad M^{(i)} \mathbf{x} = \text{vec}(\lambda_i U^{(i)T} L^{(i)} + C^{(i)} U^{(i)T}) + A^{(i)} \mathbf{x}.$$

²The subscript “tr”, indicating the “training set”, refers to the revealed entries.

Algorithm 4.2 AltMin-CG for solving (3.1)

Input: Observed tensor $\mathcal{P}_\Omega(\mathcal{T})$, graph Laplacian $\mathbf{Lap}^{(1)}, \dots, \mathbf{Lap}^{(k)}$, observed set Ω , parameters $\lambda_1, \dots, \lambda_k$ and λ_L

Output: $(U_t^{(i)})_{i=1, \dots, k}$

```

1: Initialization:  $U_0^{(1)}, \dots, U_0^{(k)}$ 
2: for  $t = 0, 1, 2, \dots$  do
3:   if stopping criterion is satisfied then
4:     return;
5:   end if
6:   for  $i = 1, \dots, k$  do
7:     Compute:  $C^{(i)}, Q^{(i)}$  defined in (4.9), (4.4b) and  $(U^{(j)})^{\odot_{j \neq i}}$ 
8:      $\mathbf{x}_{t+1}^{(i)} := \arg \min_{\mathbf{x}} g^{(i)}(\mathbf{x})$  by Algorithm 4.3
9:      $U_{t+1}^{(i)} = \text{unvec}(\mathbf{x}_{t+1}^{(i)})$ 
10:  end for
11: end for

```

Define $\text{vec}(N^{(i)}) = A^{(i)} \mathbf{x}$ with $n_{:,j}^{(i)} = A_j^{(i)} (u_{j,:}^{(i)})^\top$. Note that since m_i can be very large in practice and motivated by [48], $A_j^{(i)} (u_{j,:}^{(i)})^\top$ can be computed in the following way

$$(4.14) \quad n_{:,j}^{(i)} = A_j^{(i)} (u_{j,:}^{(i)})^\top = \sum_{\ell \in \Omega_j^{(i)}} d_{\ell,:} (u_{j,:}^{(i)})^\top d_{\ell,:}^\top.$$

Details to compute the Hessian-vector product in the CG method are listed in Algorithm 4.4.

Computational cost of AltMin-CG. The computational cost for each alternating step (4.2) corresponds to the procedure required by line 7–line 9 of Algorithm 4.2.

The cost of forming $(U^{(j)})^{\odot_{j \neq i}}$ is $O(\frac{|\Omega|R}{\rho m_i})$, where ρ denotes the sampling rate. The cost of computing $Q^{(i)}$ in (4.4b) is $O(|\Omega|R)$ with access to $(U^{(j)})^{\odot_{j \neq i}}$. The cost of forming $C^{(i)}$ in (4.9) is $O(\frac{|\Omega|R}{\rho m_i m_j})$.

The major cost in Algorithm 4.2 corresponds to line 8, which involves (inner) iterations of the linear CG. The total cost of line 8 is n_{CG} times the per-iteration cost of the linear CG algorithm (Algorithm 4.3), where n_{CG} denotes the number of iterations required by the CG solver (Algorithm 4.3) for producing $\mathbf{x}_{t+1}^{(i)}$. The per-iteration cost of Algorithm 4.3 is mainly composed of the following components.

- Cost of computing $A^{(i)} \mathbf{x}$: $O(|\Omega|R)$, since the cost of computing $A_j^{(i)} (u_{j,:}^{(i)})^\top$ in (4.14) is $O(|\Omega_j^{(i)}|R)$ for $j = 1, \dots, m_i$ and $\sum_{j=1, \dots, m_i} |\Omega_j^{(i)}| = |\Omega|$;
- Cost of computing $(L^{(i)} \otimes I_R) \mathbf{x}$: $O(\text{nnz}(L^{(i)})R)$;
- Cost of computing $(I_{m_i} \otimes C^{(i)}) \mathbf{x}$: $O(m_i R)$.

Overall, the cost of computing the Hessian-vector multiplication $M^{(i)} \mathbf{x}$ is

$$O(\text{nnz}(L^{(i)})R + |\Omega|R).$$

Algorithm 4.3 Linear CG for solving $\min g^{(i)}(\mathbf{x})$ defined in (4.3)

Input: $M^{(i)} \in \mathbb{R}^{m_i R \times m_i R}$, $Q^{(i)} \in \mathbb{R}^{m_i \times R}$, initial point $\mathbf{x}_0 \in \mathbb{R}^{m_i R}$, accuracy parameter ϵ , iteration budget T_{\max}

Output: $\mathbf{x}^* \in \mathbb{R}^{m_i R}$

```

1:  $\mathbf{r}_0 = \text{vec}(Q^{(i)}) - M^{(i)}\mathbf{x}_0$ 
2: for  $t = 0, \dots, T_{\max}$  do
3:   Compute:  $\|\mathbf{r}_t\|$ 
4:   if  $\|\mathbf{r}_t\| \leq \epsilon\|\mathbf{r}_0\|$  then
5:     Break
6:   end if
7:   if  $t = 0$  then
8:      $\mathbf{p}_1 = \mathbf{r}_0$ 
9:   else
10:     $\mathbf{p}_{t+1} = \mathbf{r}_t + \frac{\|\mathbf{r}_t\|^2}{\|\mathbf{r}_{t-1}\|^2}\mathbf{p}_t$ 
11:   end if
12:   Compute:  $\mathbf{v}_{t+1} = M^{(i)}\mathbf{p}_{t+1}$  # see Algorithm 4.4
13:   Compute:  $\alpha = \frac{\|\mathbf{r}_t\|^2}{\mathbf{p}_{t+1}^\top \mathbf{v}_{t+1}}$ 
14:   Compute:  $\mathbf{x}_{t+1} = \mathbf{x}_t + \alpha\mathbf{p}_{t+1}$ ,  $\mathbf{r}_{t+1} = \mathbf{r}_t - \alpha\mathbf{v}_{t+1}$ 
15: end for
16: return  $\mathbf{x}^* = \mathbf{x}_t$ .
```

Algorithm 4.4 Hessian-vector multiplication $M^{(i)}\mathbf{x}$ in the CG method

Input: $L^{(i)} \in \mathbb{R}^{m_i \times m_i}$, $\Omega_j^{(i)}$, $C^{(i)} \in \mathbb{R}^{R \times R}$, $D^{(i)} = (U^{(j)})^{\odot_{j \neq i}} \in \mathbb{R}^{m_{(-i)} \times R}$, $\mathbf{x} := \text{vec}(U^{(i)\top}) \in \mathbb{R}^{m_i R}$, $\lambda_i \geq 0$.

Output: $M^{(i)}\mathbf{x}$

```

1: for  $i = 1, \dots, k$  do
2:    $X = \text{unvec}(\mathbf{x}) \in \mathbb{R}^{R \times m_i}$ 
3:   Compute:  $n_{:,j}^{(i)} = \sum_{\ell \in \Omega_j^{(i)}} (d_{\ell,:} x_{:,j}) d_{\ell,:}^\top$ 
4:   Compute:  $M^{(i)}\mathbf{x} = \text{vec}(C^{(i)}X + \lambda_i X L^{(i)}) + \text{vec}(N^{(i)})$  defined in (4.13)
5: end for
```

Therefore, the dominant term in the per-iteration cost of Algorithm 4.2 is

$$(4.15) \quad n_{\text{CG}} O(\text{nnz}(L^{(i)})R + |\Omega|R).$$

Discussion. Alternating minimization (AltMin) methods have been applied to various low-rank tensor completion problems [37, 39, 40, 59] and are known for many advantages. AltMin is a desirable choice for the graph-regularized tensor decomposition problem (3.1) for the following reasons:

(i) It is easy to implement as there is no need to tune optimization parameters like step sizes; (ii) Each of the subproblems (4.2) is convex and easy to solve. In fact, we have shown in the previous subsection that each subproblem is equivalent to a least-squares problem in the $m_i R$ -dimensional

vector space; and (iii) global convergence properties of alternating minimization methods in matrix and tensor decomposition-related problems are also well known.

4.3. ADMM. Besides the AltMin-CG method, we also consider ADMM to solve the LRTC problem (3.1). ADMM becomes a very popular approach to solving a broad variety of optimization problems in signal, image processing and sparse representation problems [2, 9, 27]. The advantage of ADMM is decomposing complex optimization problems into sequences of simpler subproblems and handling of the coupling constraint by a dual multiplier. In [38], it has been illustrated that ADMM is superior over alternating least squares in terms of both reconstruction efficiency and accuracy. Furthermore, if the objective function is strongly convex and Lipschitz continuous, then linear convergence of ADMM can be achieved with a good choice of parameters [9].

We introduce $B^{(i)}$ as an auxiliary variable that equals $U^{(i)}$ to decouple the whole regularizer terms in problem (3.1) as follows

$$(4.16) \quad \min_{U^{(1)}, \dots, U^{(k)}} \frac{1}{2} \|\mathcal{P}_\Omega(\mathcal{T} - \llbracket U^{(1)}, \dots, U^{(k)} \rrbracket)\|_F^2 + \sum_{i=1}^k \frac{\lambda_i}{2} \langle B^{(i)} B^{(i)\top}, L^{(i)} \rangle + \sum_{i=1}^k \frac{\lambda_i}{2} \|(U^{(j)})^{\odot_{j \neq i}}\|_F^2,$$

subject to $U^{(i)} = B^{(i)}, i = 1, \dots, k.$

Then the augmented Lagrangian for the above optimization problem (4.16) is

$$(4.17) \quad \mathcal{L}_\eta(U, B, Y) = f(U, B) + \sum_{i=1}^k \langle Y^{(i)}, B^{(i)} - U^{(i)} \rangle + \sum_{i=1}^k \frac{\eta}{2} \|B^{(i)} - U^{(i)}\|_F^2,$$

where $f(U, B)$ denotes the objective function of (4.16) and $Y^{(i)} \in \mathbb{R}^{m_i \times R}$ is the matrix of Lagrange multiplier and $\eta > 0$ is a penalty parameter. Then apply the ADMM iterative scheme successively to minimize \mathcal{L}_η over $\{U^{(1)}, \dots, U^{(k)}\}$ and $\{B^{(1)}, \dots, B^{(k)}\}$ as follows

$$(4.18) \quad \{U_{t+1}^{(1)}, \dots, U_{t+1}^{(k)}\} = \arg \min_{\{U^{(i)}\}_{i=1}^k} \mathcal{L}_{\eta_t}(U^{(1)}, \dots, U^{(k)}, B_t^{(1)}, \dots, B_t^{(k)}, Y_t^{(1)}, \dots, Y_t^{(k)})$$

$$(4.19) \quad \{B_{t+1}^{(1)}, \dots, B_{t+1}^{(k)}\} = \arg \min_{\{B^{(i)}\}_{i=1}^k} \mathcal{L}_{\eta_t}(U_{t+1}^{(1)}, \dots, U_{t+1}^{(k)}, B^{(1)}, \dots, B^{(k)}, Y_t^{(1)}, \dots, Y_t^{(k)})$$

$$(4.20) \quad Y_{t+1}^{(i)} = Y_t^{(i)} + \eta_t(B_{t+1}^{(i)} - U_{t+1}^{(i)}), \quad i = 1, \dots, k.$$

Updating $\{U_{t+1}^{(1)}, \dots, U_{t+1}^{(k)}\}$: The optimization problem (4.18) can be rewritten as follows when updating $\{U_{t+1}^{(1)}, \dots, U_{t+1}^{(k)}\}$

$$(4.21) \quad \min_{U^{(1)}, \dots, U^{(k)}} \frac{1}{2} \|\mathcal{P}_\Omega(\mathcal{T} - \llbracket U^{(1)}, \dots, U^{(k)} \rrbracket)\|_F^2 + \sum_{i=1}^k \frac{\lambda_i}{2} \|(U^{(j)})^{\odot_{j \neq i}}\|_F^2 + \sum_{i=1}^k \frac{\eta_t}{2} \|U^{(i)} - B_t^{(i)} - (1/\eta_t)Y_t^{(i)}\|_F^2.$$

We apply the alternating minimization method to update each $U^{(i)}$ for $i = 1, \dots, k$, while fixing the other variables. Then problem (4.21) becomes a quadratic optimization problem. For convenience, we ignore the subscript in the fixed $U^{(j)}$ for $j \neq i$, and the resulting subproblem with respect to $U^{(i)}$ is

formulated as

$$(4.22) \quad \min_{U^{(i)}} \frac{1}{2} \|\mathcal{P}_{\Omega^{(i)}}(\mathcal{T}_{(i)} - U^{(i)}[(U^{(j)})^{\odot_{j \neq i}}]^\top)\|_F^2 + \sum_{\substack{j=1 \\ j \neq i}}^k \frac{\lambda_j}{2} \|(U^{(n)})^{\odot_{n \neq j}}\|_F^2 + \frac{\eta_t}{2} \|U^{(i)} - B_t^{(i)} - \frac{Y_t^{(i)}}{\eta_t}\|_F^2,$$

which is separable by rows of $U^{(i)}$. Thus, each row of the new iterate $U_{t+1}^{(i)}$ is the solution to the following linear equation in \mathbb{R}^R ,

$$(4.23) \quad (A_j^{(i)} + \eta_t I_R + C^{(i)})(U_{j,:}^{(i)})^\top = [(\mathcal{P}_{\Omega^{(i)}} \mathcal{T}_{(i)})(U^{(j)})^{\odot_{j \neq i}} + \eta_t B_t^{(i)} + Y_t^{(i)}]_{j,:}^\top,$$

where $A_j^{(i)}$ and $C^{(i)}$ are defined in (4.7) and (4.9) respectively, for $j = 1, \dots, m_i$.

Updating $\{B_{t+1}^{(1)}, \dots, B_{t+1}^{(k)}\}$: By alternating minimization method, the optimization problem (4.19) can be reformulated as follows when updating the variables $\{B_{t+1}^{(1)}, \dots, B_{t+1}^{(k)}\}$,

$$(4.24) \quad \min_{B^{(i)}} \frac{\lambda_i}{2} \langle B^{(i)} B^{(i)\top}, L^{(i)} \rangle + \frac{\eta_t}{2} \|U_{t+1}^{(i)} - B^{(i)} - (1/\eta_t) Y_t^{(i)}\|_F^2.$$

which boils down to solving

$$(4.25) \quad (\eta_t I_{m_i} + \lambda_i L^{(i)}) B^{(i)} = \eta_t U_{t+1}^{(i)} - Y_t^{(i)}.$$

Followed by the above standard procedure of ADMM, it concludes in Algorithm 4.5. Here we adopt the CG method combined with the Hessian-vector product defined in the previous subsection to update $B_{t+1}^{(i)}$ in (4.25) (also corresponding to line 10 of Algorithm 4.5). The iterate $U_{t+1}^{(i)}$ in (4.23) is updated by rows, therefore a simple CG solver is used.

Computational cost of ADMM. We analyze the computational cost for each alternating step of the augmented Lagrangian step (4.17) corresponding to the procedure required by line 6–line 12 of Algorithm 4.5. The costs of forming $(U^{(j)})^{\odot_{j \neq i}}$, $C^{(i)}$ and $Q^{(i)}$ are computed in the complexity analysis part of Section 4.2. Let n_{ADMM} denote the maximal number of iterations required for solving the linear equations (4.23) and (4.25). Then the dominant costs are $n_{\text{ADMM}} O(m_i R + |\Omega| R)$ and $n_{\text{ADMM}} O(\text{nnz}(L^{(i)}) R)$ respectively. Therefore, the total complexity of Algorithm 4.5 (ADMM) is $n_{\text{ADMM}} O(\text{nnz}(L^{(i)}) R + |\Omega| R)$, which is of the same order as Algorithm 4.2 (AltMin-CG).

5. Convergence analysis. In this section, we will show the global convergence of iterates $\{U^{(1)}, \dots, U^{(k)}\}$ generated by Algorithm 4.2 (AltMin-CG) to a critical point.

5.1. Preliminaries. The following definitions and lemmas are used for the convergence analysis in the next subsection.

Definition 5.1. [52][4, Definition 1] Let $f : \mathbb{R}^m \mapsto \mathbb{R} \cup \{+\infty\}$ be proper and lower semicontinuous.

- 1) The domain of f is defined and denoted by $\text{dom } f := \{\mathbf{x} \in \mathbb{R}^m : f(\mathbf{x}) < +\infty\}$.
- 2) For each $\mathbf{x} \in \text{dom } f$, the Fréchet subdifferential of f at \mathbf{x} , denoted as $\hat{\partial} f(\mathbf{x})$, is

$$(5.1) \quad \hat{\partial} f(\mathbf{x}) = \left\{ \xi \in \mathbb{R}^m : \liminf_{\substack{\mathbf{y} \neq \mathbf{x} \\ \mathbf{y} \rightarrow \mathbf{x}}} \frac{f(\mathbf{y}) - f(\mathbf{x}) - \langle \xi, \mathbf{x} - \mathbf{y} \rangle}{\|\mathbf{x} - \mathbf{y}\|} \geq 0 \right\}.$$

Algorithm 4.5 ADMM for problem (3.1)

Input: Observed tensor $\mathcal{P}_\Omega(\mathcal{T})$, graph Laplacian $\mathbf{Lap}^{(1)}, \dots, \mathbf{Lap}^{(k)}$, observed set Ω , parameters $\lambda_1, \dots, \lambda_k$ and λ_L

Output: $(U_t^{(i)})_{i=1, \dots, k}$

```

1: Initialization:  $U_0^{(1)}, \dots, U_0^{(k)}, \eta_0$ 
2: for  $t = 0, 1, 2, \dots$ , do
3:   if stopping criterion is satisfied then
4:     return;
5:   end if
6:   for  $i = 1, \dots, k$  do
7:     for  $j = 1, \dots, m_i$  do
8:       Update the  $j$ -th row of  $U_{t+1}^{(i)}$  by (4.23)
9:     end for
10:    Update  $B_{t+1}^{(i)}$  by (4.25)
11:     $Y_{t+1}^{(i)} = Y_t^{(i)} + \eta_t^{(i)}(B_{t+1}^{(i)} - U_{t+1}^{(i)})$ 
12:  end for
13:  Update  $\eta_{t+1} = \gamma \eta_t$ 
14: end for

```

If $\mathbf{x} \notin \text{dom} f$, then $\hat{\partial} f(\mathbf{x}) = \emptyset$.

3) The limiting subdifferential of f at $\mathbf{x} \in \text{dom} f$, denoted as $\partial f(\mathbf{x})$, is defined as follows [43]

$$(5.2) \quad \partial f(\mathbf{x}) := \{\xi^* \in \mathbb{R}^m : \exists (\mathbf{x}_n)_{n \geq 0}, \mathbf{x}_n \rightarrow \mathbf{x}, f(\mathbf{x}_n) \rightarrow f(\mathbf{x}), \text{ s.t. } \exists \xi_n \in \hat{\partial} f(\mathbf{x}_n), \xi_n \rightarrow \xi^*\}.$$

Definition 5.2 (KŁ function). [59, Definition 2.5] A function $f(\mathbf{x})$ satisfies the Kurdyka-Łojasiewicz (KŁ) property at point $\bar{\mathbf{x}} \in \text{dom}(\partial f)$ if, in a certain neighborhood \mathcal{U} of $\bar{\mathbf{x}}$, there exists $\psi(s) = cs^{1-\theta}$ for some $c > 0$ and $\theta \in [0, 1)$ such that the KŁ inequality below holds:

$$(5.3) \quad \psi'(f(\mathbf{x}) - f(\mathbf{x}^*)) \text{dist}(0, \partial f(\mathbf{x})) \geq 1, \text{ for any } \mathbf{x} \in \mathcal{U} \cap \text{dom}(\partial f) \text{ and } f(\mathbf{x}) \neq f(\mathbf{x}^*),$$

where $\text{dom}(\partial f) = \{\mathbf{x} : \partial f(\mathbf{x}) \neq \emptyset\}$ and $\text{dist}(0, \partial f(\mathbf{x})) = \min\{\|\mathbf{y}\| : \mathbf{y} \in \partial f(\mathbf{x})\}$.

If f satisfies the KŁ property at each point of $\text{dom}(f)$, f is called a KŁ function.

Definition 5.3 (Strong convexity). A differentiable function $f : \text{dom} f \mapsto \mathbb{R}$ is strongly convex if and only if

$$(5.4) \quad f(\mathbf{y}) \geq f(\mathbf{x}) + \langle \nabla f(\mathbf{x}), \mathbf{y} - \mathbf{x} \rangle + \frac{\mu}{2} \|\mathbf{y} - \mathbf{x}\|^2$$

holds for some $\mu > 0$ and all $\mathbf{x}, \mathbf{y} \in \text{dom} f$.

Definition 5.4 (Coercivity). A real-valued function $f : \mathbb{R}^m \rightarrow \mathbb{R}$ is called coercive if and only if

$$(5.5) \quad f(\mathbf{x}) \rightarrow +\infty \quad \text{as} \quad \|\mathbf{x}\| \rightarrow +\infty.$$

The following two lemmas follow directly from Theorem 2.8 and Theorem 2.9 of [59] and are used for proving the convergence of the proposed alternating minimization method.

Lemma 5.5. *Assume f satisfies the KŁ property and ∇f is Lipschitz continuous on any bounded subset of its domain. Let $(U_0^{(1)}, \dots, U_0^{(k)})$ be any initialization and $(U_t^{(1)}, \dots, U_t^{(k)})$ be the sequence generated by Algorithm 4.1, where each subproblem $f_t^{(i)}(U^{(i)})$ (line 7 of Algorithm 4.1) is strongly convex and is solved exactly. If the sequence $(U_t^{(1)}, \dots, U_t^{(k)})$ is bounded and there exists a finite limit point $(U_*^{(1)}, \dots, U_*^{(k)})$, then it converges to $(U_*^{(1)}, \dots, U_*^{(k)})$, which is a critical point of f .*

The convergence rate of the sequence is as follows.

Lemma 5.6. *Assume ∇f is Lipschitz continuous on any bounded set and suppose that $U_t^{(i)}$ converges to a critical point $U_*^{(i)}$ for $i = 1, \dots, k$, at which f satisfies the KŁ inequality with $\psi(s) = cs^{1-\theta}$ for $c > 0$ and $\theta \in [0, 1)$. We have:*

1. *If $\theta = 0$, $U_t^{(i)}$ converges to $U_*^{(i)}$ in a finite number of iterations;*
2. *If $\theta \in (0, \frac{1}{2}]$, $\|U_t^{(i)} - U_*^{(i)}\| \leq \beta\tau^t$, $\forall t \geq t_0$ for certain $t_0 > 0$, $\beta > 0$, $\tau \in [0, 1)$;*
3. *If $\theta \in (\frac{1}{2}, 1)$, $\|U_t^{(i)} - U_*^{(i)}\| \leq \beta t^{-(1-\theta)/(2\theta-1)}$, $\forall t \geq t_0$ for certain $t_0 > 0$, $\beta > 0$.*

Part 1, 2 and 3 correspond to finite convergence, linear convergence, and sublinear convergence, respectively.

5.2. Convergence properties of AltMin. We show that the iterates generated by Algorithm 4.1 (AltMin) converge to a stationary point in the following theorem. Note that this theorem applies to Algorithm 4.2 (AltMin-CG), provided that the updated iterate of each of the subproblems (line 8 in Algorithm 4.2) is the exact minimizer of the corresponding (graph-regularized) least-squares problem. In practice, this requires setting a sufficiently low tolerance parameter ϵ for the subproblem solver (Algorithm 4.3).

Theorem 5.7. *The iterates $(U_t^{(1)}, \dots, U_t^{(k)})$ generated by Algorithm 4.1 (AltMin) from any initialization converge globally to a critical point of f in (3.1). Moreover, linear convergence and sublinear convergence in parts 2 and 3 of Lemma 5.6 apply depending on θ in KŁ property of f .*

Proof. According to Lemma 5.5, we need to check whether all the assumptions satisfied.

1) Function f in (3.1) is a KŁ function with $\theta \in [1/2, 1)$ as it is a combination of polynomials which are one kind of real analytic functions (see [34, Definition 1.1.5]). The real analytic function itself and the finite sum or product of real analytic functions are KŁ functions, see [4, section 4] and [59, section 2.2].

2) Gradient ∇f is Lipschitz continuous on any bounded subset of domain since f is a C^∞ function.

3) For $i = 1, \dots, k$, $f^{(i)}$ in (4.2) is strongly convex by Definition 5.3 since $L^{(i)}$ in (3.2) is positive definite. Therefore, the quadratic form $g^{(i)}$ of the subproblems (4.3) is strongly convex through the identification $g^{(i)}(\text{vec}(U^{(i)\top})) = f^{(i)}(U^{(i)})$. Moreover, the solution for each $g^{(i)}$ corresponds to the exact minimizer.

4) Notice that since f is coercive as defined in Definition 5.4 and real analytic, it is guaranteed to produce a bounded sequence $(U_t^{(1)}, \dots, U_t^{(k)})$, thus it has a critical point $(U_*^{(1)}, \dots, U_*^{(k)})$.

Lemma 5.5 then implies that the sequence generated by Algorithm 4.2 from any initial point converges to a critical point $(U_*^{(1)}, \dots, U_*^{(k)})$ of f . Moreover, the asymptotic convergence rates in

parts 2 and 3 of Lemma 5.6 apply as $\theta \in [1/2, 1)$. ■

6. Experiments. In this section, we carry out some numerical experiments to demonstrate the working of our proposed algorithms Algorithm 4.2 (AltMin-CG) and Algorithm 4.5 (ADMM) on the LRTC model (3.1) with $k = 3$. All numerical experiments were performed on a Macbook Pro with a 2.3 GHz Intel Core i7 CPU, 16GB RAM and MATLAB R2015a with Tensor Toolbox version 2.5 [5]. The source code is made available online.³

We focus on the following two tasks:

1. To test and verify the effect of the graph Laplacian-based regularizer in our model (3.1), we compare the recovery quality of solutions given by the graph-regularized tensor completion model with two graph-agnostic tensor completion models.
2. To validate the effectiveness and efficiency of the proposed methods Algorithm 4.2 and Algorithm 4.5 when applied to solving model 3.1, we compare with other baseline methods on both synthetic data and real data.

In our experiments, we evaluate the quality of a tensor approximation with the following error functions, for a given index set Ω' that contains only the known entries of \mathcal{T}^* : (i) the relative error (RE) of the tensor candidate $\mathcal{T} = \llbracket U^{(1)}, \dots, U^{(k)} \rrbracket$ against \mathcal{T}^* on Ω' in the Frobenius norm, and (ii) the root mean squared error (RMSE) of \mathcal{T} restricted on Ω' . The training and test RMSEs refer to the RMSE on the training and test set respectively.

Initialization. We initialize both our proposed methods and other methods with a point $U_0 \in \mathbb{R}^{m_1 \times R} \times \mathbb{R}^{m_2 \times R} \times \mathbb{R}^{m_3 \times R}$ where each factor matrix $U_0^{(i)}$ is a Gaussian matrix such that $[U_0^{(i)}]_{jr} \sim \mathcal{N}(0, 1)$.

Experimental methodology. Based on a ground truth tensor $\mathcal{T} \in \mathbb{R}^{m_1 \times m_2 \times m_3}$ and for a fixed sampling rate ρ , we generate N_{test} training instances $(\Omega_\ell)_{\ell=1, \dots, N_{\text{test}}}$ under the same sampling rate ρ . For each training instance $(\mathcal{T}, \Omega_\ell)$, N_{init} initial points $(U_{0,(\ell,j)})$, for $j = 1, \dots, N_{\text{init}}$, are generated. Let $\hat{\mathcal{T}}(U_{0,(\ell,j)}; \Omega_\ell)$ denote the solution of the j -th test based on the training instance $(\mathcal{T}, \Omega_\ell)$ with the initial point $U_{0,(\ell,j)}$, and $E(\hat{\mathcal{T}})$ the error (e.g., RE, RMSE) of the candidate tensor $\hat{\mathcal{T}}$ w.r.t. \mathcal{T} . Then each method is evaluated by the following score

$$(6.1) \quad \text{Err} = \frac{1}{N_{\text{test}} N_{\text{init}}} \sum_{\ell=1}^{N_{\text{test}}} \sum_{j=1}^{N_{\text{init}}} E(\hat{\mathcal{T}}(U_{0,(\ell,j)}); \Omega_\ell).$$

In all experiments we select $N_{\text{test}} = 5$ and $N_{\text{init}} = 10$.

Parameter selection. In all experiments, the problem-related parameters (λ_i, λ_L) in (3.1)–(3.2) are generated randomly with the uniform distribution in the log scale. Then the parameter is chosen among all generated parameter settings through K -fold cross validation (for $K = 3$).

6.1. Graph-regularized and graph-agnostic tensor completion models. In this subsection, we conduct tests to compare the graph-regularized tensor completion model with graph-agnostic models. Hereafter, we refer to our graph-regularized tensor completion model (3.1) as GREG-TC, when λ_i and λ_L are nonzero. The model (3.1) is referred to as NUCLREG-TC when the problem parameter for the graph Laplacian-based regularization term is reduced to zero, i.e., $\lambda_L = 0$, but the

³ <https://gitlab.com/ricky7guanyu/tensor-completion-with-regularization-term>.

Sample Ratio	Algorithm	GREG-TC	NUCLREG-TC	UNREG-TC
0.3%	AltMin-CG	0.8198	1.0083	7.1110
	ADMM	0.8246	1.0054	4.4393
0.5%	AltMin-CG	0.4418	0.9201	9.9010
	ADMM	0.4486	0.9236	7.6692
0.7%	AltMin-CG	0.3106	0.7561	9.9548
	ADMM	0.3000	0.7487	8.4821
1%	AltMin-CG	0.1380	0.4772	13.5740
	ADMM	0.1439	0.4513	10.9230

Table 1

Average recovery accuracies (relative error) of the three models on synthetic data: GREG-TC (with graph Laplacian), NUCLREG-TC (without graph Laplacian), UNREG-TC (no regularizer).

other regularizers are kept active (λ_i nonzero). The model (3.1) is referred to as UNREG-TC when all regularization parameters are reduced to zero, i.e., $\lambda_i = \lambda_L = 0$.

In the experiments of this subsection, the stopping criteria consist of (i) a large iteration budget parameter T_{\max} ; and (ii) a global tolerance parameter ϵ for (4.12).

Experiment on synthetic data with graph information. As our model (3.1) has a graph regularizer term, it is tempting to generate a synthetic low rank tensor \mathcal{T} that features some graph information inside.

Here is how we construct such a synthetic tensor. First, we generate the graph Laplacian matrix $\mathbf{Lap}^{(1)} \in \mathbb{R}^{100 \times 100}$ of $U^{(1)}$ which exhibits row-wise similarities by the prototypical graph model "Community" using GSPbox [46]. Let $\mathbf{Lap}^{(1)} = \bar{U} \bar{\Lambda} \bar{U}^\top$ be the eigenvalue value decomposition of a given graph Laplacian matrix. We consider the following tensor model,

$$\mathcal{T} = \llbracket \tilde{A} U^{(1)}, U^{(2)}, U^{(3)} \rrbracket + \mathcal{E},$$

where $\tilde{A} = \bar{U} \bar{\Lambda}^{-1}$ and $(U^{(1)}, U^{(2)}, U^{(3)}) \in \mathbb{R}^{m_i \times R}$ are random matrices whose columns are i.i.d. Gaussian vectors. The tensor \mathcal{E} contains additive noise such that $\mathcal{E}_{\ell_1 \ell_2 \ell_3} \sim \mathcal{N}(0, \sigma)$, where σ is set according to a given signal-to-noise ratio (SNR). In this experiment, we set SNR to 20 dB. The graph information is incorporated in the tensor model as follows. By construction, the first factor matrix belongs to an eigensubspace of a given graph Laplacian matrix with a prescribed order of "preferences" for each of the eigenvectors (here the preferences are given by $(1/\bar{\lambda}_i)_{i=1, \dots, R}$). Here, the model enables building a tensor where the entries along the first dimension exhibit pairwise similarities according to the connections of the given graph. This model can be seen in the related work on graph-based regularization for matrix completion [47, 21].

We test various sample rates (SR) in $\{0.3\%, 0.5\%, 0.7\%, 1\%\}$. The average relative errors (RE) are listed in Table 1. Figure 1 shows the histogram of $SR = 0.3\%$, and other histograms are put in Figures 9, 10 and 11 in the supplementary material. We see that on this experiment, our GREG-TC model outperforms both other models, for both tested methods.

6.1.1. Real data. Next, we consider experimenting from two real-world datasets. An essential difference between these experiments and the experiments on synthetic data is that there is no ground-

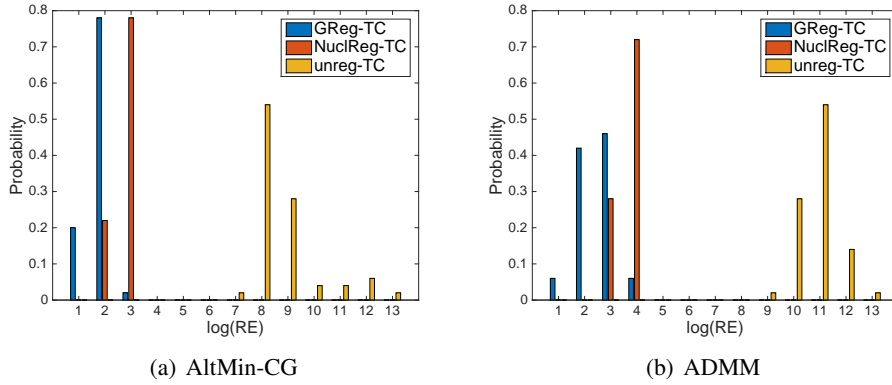


Figure 1. Recovery accuracies of the three tensor completion models on synthetic data. The sampling rate $SR = 0.3\%$.

truth similarity graphs associated with the data tensor. While we assume that real life data often present pairwise similarities between its entries, we need to build the graph Laplacians $\mathbf{Lap}^{(i)}$.

Experiment on the MovieLens dataset. We now evaluate the models on a movie rating dataset called MovieLens dataset 100k,⁴ which consists of 100,000 movie ratings from 943 users on 1682 movies during a seven-month period from September 19th, 1997 through April 22nd, 1998. Each movie rating in this dataset has a time stamp. Therefore, we obtain a tensor \mathcal{T} of size $943 \times 1682 \times 7$ (*i.e.*, time period is split into 7 parts). We randomly select 80% of the known ratings as training set.

In this experiment, we construct a movie-wise similarity graph based on the data matrix itself (with missing entries). Let M^* denote the MovieLens data matrix with missing entries. We compute the graph proximity parameters based on a low-rank approximation of the partially revealed matrix. More precisely, we use a rank- r approximation of the zero-filled matrix $M_0 := P_\Omega(M^*) \in \mathbb{R}^{m \times n}$ as the features for constructing the graph. Let (U_0, S_0, V_0) denote the r -SVD of M_0 and let $\tilde{M}_0 := U_0 S_0 V_0^T$.

Next, the computation of the graph edge weight parameters based on the given matrix $M := \tilde{M}_0$ can be realized using various node proximity methods such as K -Nearest Neighbors (K -NN) and ε -graph models [14, 7, 29, 15], which boil down to computing a certain distance matrix between the rows (resp. columns) of M . Let $Z^r(M) \in \mathbb{R}^{m \times m}$ denote the row-wise distance matrix of M defined as $Z_{ij}^r(M) = d(M_{i,:}, M_{j,:})$, for $i, j \in \llbracket m \rrbracket$, where $d: \mathbb{R}^n \times \mathbb{R}^n \mapsto \mathbb{R}_+$ is a distance on the n -dimensional vector space. Subsequently, we build a Gaussian ε -graph by computing the node proximity weights as follows

$$(6.2) \quad [W_\varepsilon(M)]_{ij} = \exp\left(-Z_{ij}^r(M)/\varepsilon^2\right), \text{ for } i, j \in \llbracket m \rrbracket,$$

where $\varepsilon \in \mathbb{R}$ is a hyperparameter of the graph model. Furthermore, a sparse graph adjacency matrix is preferable to a dense one from a computational point of view, as the per-iteration cost of the proposed algorithms (*e.g.* Algorithm 4.2) depends partly on $\text{nnz}(L^r)$ and $\text{nnz}(L^c)$. For simplicity, we sparsify the graph adjacency matrix defined in (6.2) with the following thresholding operation

$$(6.3) \quad [W_{\varepsilon,\sigma}(M)]_{ij} = \mathbf{1}_{\geq \sigma} \left(\exp\left(-Z_{ij}^r(M)/\varepsilon^2\right) \right), \text{ for } i, j \in \llbracket m \rrbracket,$$

⁴<https://grouplens.org/datasets/movielens/100k/>

Method	GREG-TC	NUCLREG-TC	UNREG-TC
AltMin-CG	0.2233	0.2233	1.4526
ADMM	0.2193	0.2234	1.1205

Table 2

RE of the three models on the MovieLens dataset: GREG-TC (with graph Laplacian), NUCLREG-TC (without graph Laplacian), UNREG-TC (no regularizer).

where $\mathbf{1}_{\geq\sigma}$ is the hard threshold function $\mathbf{1}_{\geq\sigma}(z) = \begin{cases} z & \text{if } z \geq \sigma \\ 0 & \text{otherwise.} \end{cases}$

In the graph model (6.3), parameter ε is tuned according to the variance of $(Z_{ij})_{i,j=1,\dots,m}$ and threshold σ is chosen according to a preset sparsity level $\varepsilon \ll 1$ for the edge set associated with $W_{\varepsilon,\sigma}$ such that $|\mathcal{E}(W_{\varepsilon,\sigma})|/m^2 \leq \varepsilon$.

The results of average RE after running 50 times with random initializations are listed in Table 2, while the histogram of these results is presented in Figure 2. These results show that the solutions to the graph-regularized model (3.1) (labeled GREG-TC) and NUCLREG-TC model have better recovery performance (in terms of RMSE) than UNREG-TC model. The gain of recovery performance induced by the graph learned from the data may be considered marginal; however, on movie rating data, it is notoriously difficult to improve the RMSE score much beyond basic methods [8].

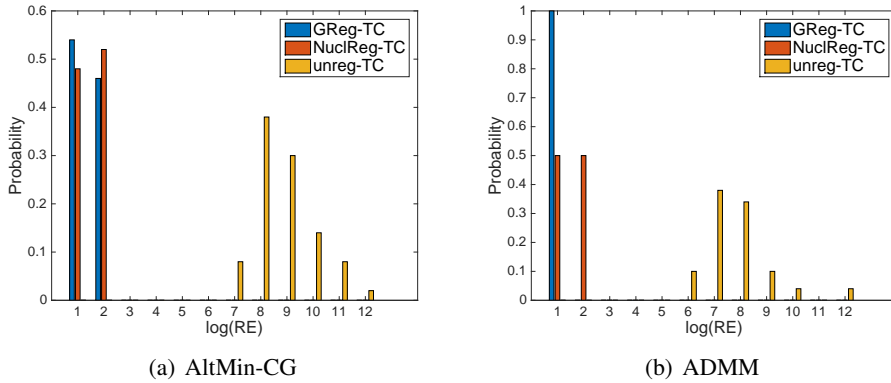


Figure 2. Recovery accuracies (relative error) of the three tensor completion models on the MovieLens dataset.

Experiment on the FIA dataset. In this experiment, we use the “rank-deficient spectral FIA dataset”.⁵ This dataset consists of results of flow injection analysis on 12 different chemical substances. The represented tensor is of size 12(substances) \times 100(wavelengths) \times 89(reaction times). We construct the adjacency matrices following the ideas in [44, Section 4.1]. For 12 chemical substances, we build the adjacency matrix between two substances as the inverse of Euclidean distance between their feature vectors. For wavelengths and reaction times, the adjacency matrices are built using the simple chain graph model since these quantities varies in a smooth manner in their respective domains of definition.

⁵<http://www.models.life.ku.dk/datasets>

Sample Ratio	Algorithm	GREG-TC	NUCLREG-TC	UNREG-TC
1%	AltMin-CG	0.1012	1.1096	6.6597
	ADMM	0.2396	1.1385	1.5985
5%	AltMin-CG	0.0146	0.3470	3.9619
	ADMM	0.0209	0.2131	0.2131
7%	AltMin-CG	0.0126	0.2087	0.3837
	ADMM	0.0180	0.0572	0.0572

Table 3

RE of the three models on the FIA dataset: GREG-TC (with graph Laplacian), NUCLREG-TC (without graph Laplacian), UNREG-TC (no regularizer).

The sample ratio varies the fraction of observed entries as 1%, 5% and 7%. We present in Table 3 average results after running 50 times, the histogram for $SR = 1\%$ is in Figure 3, and other histograms are listed in Figures 12 and 13 in the supplementary material. Similar to the comparative results on synthetic data, these results show that the solutions of the GREG-TC model have smaller recovery errors compared to those of the other two models.

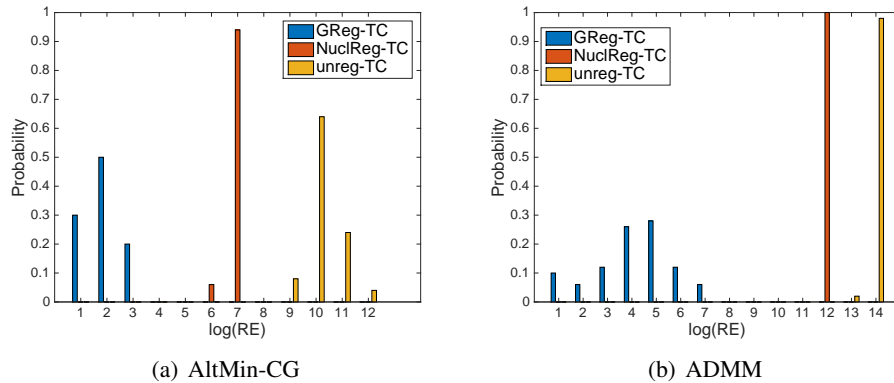


Figure 3. Recovery accuracies (relative error) of the three tensor completion models on the FIA dataset. The sampling rate $SR = 1\%$.

Observations and results The results in Tables 1–3 show that the solutions of the graph-regularized model (3.1) (labeled by GREG-TC) have smaller recovery errors than those of the two graph-agnostic models, NUCLREG-TC and UNREG-TC. This observation is encouraging since it indicates that incorporating graph auxiliary information in the tensor completion model leads to more robust recovery results, especially when the proportion (sampling rate) of the revealed entries is very low.

In particular, the lack of regularization poses issues on the robustness and stability of the solutions under “small sampling rates”: One can see that in the range of sampling rates tested, the recovery accuracy of solutions given by the graph-agnostic models (UNREG-TC and NUCLREG-TC) do not necessarily improve with an increasing sampling rate. The iterative results (Figure 14 in the supplementary material) of AltMin for solving the UNREG-TC model on synthetic data provide an intuitive explanation: Under these sampling rates and the unregularized model, the recovery error of the iter-

ates on unrevealed entries (the test error) does not decrease (and increases on the contrary) in spite of the decreasing error on the revealed entries (training error). In other words, under these insufficient sampling rates, a smaller training error does not imply an improved test error.

The graph Laplacians in synthetic data are comparably easy to build using the synthetic data itself, which always has the ground truth. In comparison, for real data, we need to explore and construct the adjacency matrix from the observed data, which is only a small portion of the data. Moreover, sometimes the data itself is not well collected. Notice that in the MovieLens experiment, we build the graph Laplacians only in user mode without metadata about the background information of users. Therefore, the GREG-TC and NUCLREG-TC models perform relatively similar, and both demonstrate lower relative errors. With the increase of the sample ratio, the effect of graph Laplacians is getting weaker as shown in Table 3.

Moreover, from histograms, we find that the proposed GREG-TC model and NUCLREG-TC model display better consistency than the UNREG-TC model, as the results of 50 runs are quite close, implying that the proposed model is more robust on predicting the missing data. The last values of $\log(\text{RE})$ in the GREG-TC model always stay at the same bar or at the adjacent bar, and are located left of those of the NUCLREG-TC model and UNREG-TC model.

6.2. Evaluating the time efficiency of proposed algorithms. In this subsection, we focus on evaluating the time efficiency of our proposed algorithms under the same experimental settings described in the last subsection. In each of the following experiments, iteration information for our proposed algorithms is recorded. At each iteration, the recovery quality of the current iterate is evaluated in terms of the RMSE on test entries.

Besides our proposed algorithms, a representative selection of state-of-art methods are also tested, based on their codes that are publicly available or made available to us: (i) INDAFAC is a damped Gauss-Newton method proposed by Tomasi and Bro [56] for solving the following tensor completion model

$$\min_{\mathcal{T}, U} \|\mathcal{T}_{(1)} - U^{(1)}(U^{(3)} \odot U^{(2)})^\top\|_F^2 \text{ s.t. } \mathcal{P}_\Omega(\mathcal{T} - \mathcal{Z}) = \mathbf{0},$$

where \mathcal{Z} is only known on Ω ; (ii) CP-WOPT [1] is an algorithm for solving the CPD-based problem $\min_U \|P_\Omega(\llbracket U^{(1)}, U^{(2)}, U^{(3)} \rrbracket) - \mathcal{T}^*\|_F^2$ and is available in the Tensor Toolbox [5]; (iii) BPTF is a Bayesian probabilistic tensor CPD algorithm [58] and solves a regularized problem

$$\min_U \|P_\Omega(\llbracket U^{(1)}, U^{(2)}, U^{(3)} \rrbracket) - \mathcal{T}^*\|_F^2 + \psi(U)$$

where the regularizer ψ is composed of Frobenius norms of the factors of U and a ℓ_2 norm-based function imposing columnwise smoothness of $U^{(3)}$; (iv) TFAI [44] is an algorithm for tensor completion with auxiliary information. We adopt the within-mode auxiliary information method with the graph Laplacians shown as

$$\min_{\mathcal{T}, U} \|\mathcal{T} - \llbracket U^{(1)}, U^{(2)}, U^{(3)} \rrbracket\|_F^2 + \psi(U) \text{ s.t. } \mathcal{P}_\Omega(\mathcal{T}) = \mathcal{P}_\Omega(\mathcal{T}^*),$$

where ψ is a graph Laplacian-based regularizer as in (3.1); (v) TNCP [41] is an ADMM algorithm for

solving the following matrix trace-norm regularized problem

$$\min_{\mathcal{T}, U} \frac{\lambda}{2} \|\mathcal{T} - \llbracket U^{(1)}, U^{(2)}, U^{(3)} \rrbracket\|_F^2 + \sum_{i=1}^3 \alpha_i \|U^{(i)}\|_* \text{ s.t. } \mathcal{P}_\Omega(\mathcal{T}) = \mathcal{P}_\Omega(\mathcal{T}^*);$$

and (vi) AirCP [25] is an ADMM algorithm for solving the CP-based tensor completion using auxiliary graph information

$$\min_{\mathcal{T}, U, X} \frac{\lambda}{2} \|\mathcal{T} - \llbracket U^{(1)}, U^{(2)}, U^{(3)} \rrbracket\|_F^2 + \psi(U, X) \text{ s.t. } \mathcal{P}_\Omega(\mathcal{T}) = \mathcal{P}_\Omega(\mathcal{T}^*), U^{(i)} = X^{(i)},$$

$\psi(U, X)$ is composed of the sum of Frobenius norms of $U^{(i)}$ and the graph Laplacian-based norms of $X^{(i)}$.

Remark 6.1. The parameters involved in the models of TFAI, TNCP and AirCP are chosen after cross validation.

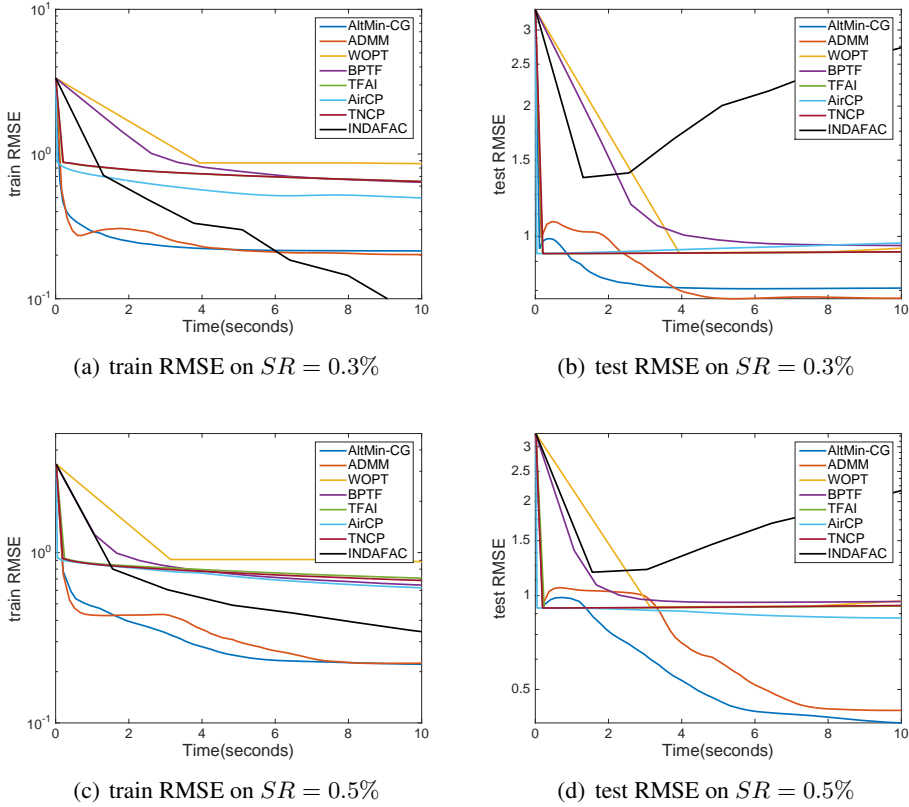


Figure 4. Iterative results of the tested algorithms on synthetic data: RMSE on training and test sets by accumulative time per-iteration. The sampling rates tested are 0.3% and 0.5%.

Experiment on synthetic data with graph information. Under the same experimental settings as for Table 1, the RMSEs of the iterates given by the tested methods are shown in Figure 4 (and Figure 7 in the supplementary material). The iterative results in the figures are taken from one test randomly chosen from the repeated tests. Figure 4 shows the results under the sampling rates $SR = 0.3\%$ and 0.5% , in which we observe that proposed algorithms, AltMin-CG and ADMM, have a better time efficiency than the rest of the tested methods. Detailed observations on these results are given in Section 6.2.1.

Experiment on the MovieLens dataset. Under the same experimental settings on the MovieLens dataset and with the same graph construction method as in the previous subsection, we show the RMSEs of the iterates given by the tested methods in Figure 5. The iterative results in the figure are taken from one test randomly chosen from the repeated tests. In particular, the labels “AltMin-CG1” and “ADMM1” represent the results of these algorithms under the graph-agnostic, nuclear norm-based model (NuclReg-TC). The results therein shows that the AltMin-CG and ADMM methods remain competitive on this dataset, in particular their time efficiency is comparable to AirCP.

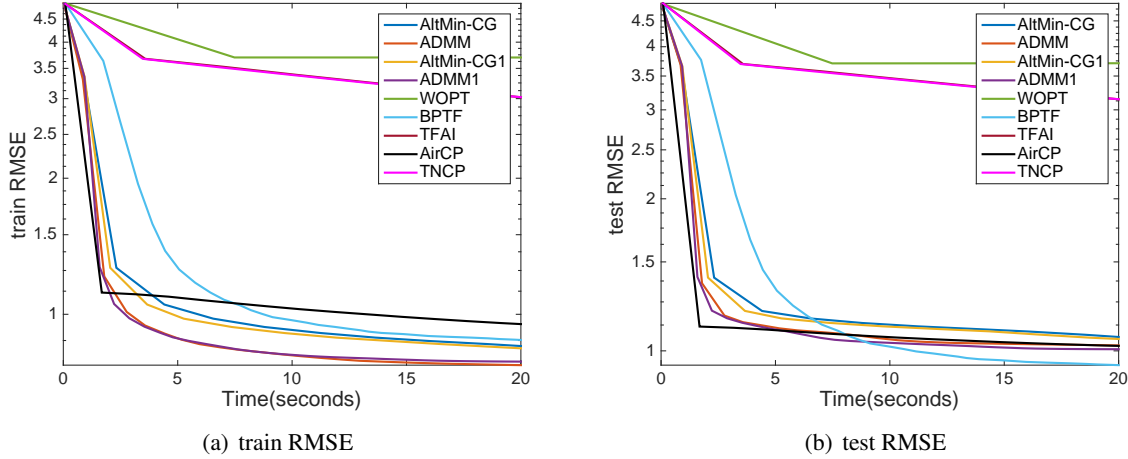


Figure 5. Iterative results of the tested algorithms on the MovieLens dataset: RMSE on training and test sets by accumulative time per-iteration.

Experiment on the FIA dataset. Under the same experimental settings on the FIA dataset and with the same graph construction method as in the previous subsection, we show the RMSEs of the iterates given by the tested methods in Figure 6. The iterative results in the figure are taken from one test randomly chosen from the repeated tests. These results show that the proposed algorithms AltMin-CG and ADMM yield the best recovery performances (in terms of test RMSE).

6.2.1. Observations and results. From Figure 4 and Figure 7, we observe that most of the methods perform comparably in time efficiency. In particular, the proposed AltMin-CG and ADMM methods, followed by AirCP, TFAI, TNCP, are the fastest in terms of training RMSE. Also, AltMin-CG and ADMM achieve the lowest test RMSEs, under low sampling rates. This result is encouraging since it shows that our methods and model for tensor completion can achieve robust recovery where only a small fraction of data is available.

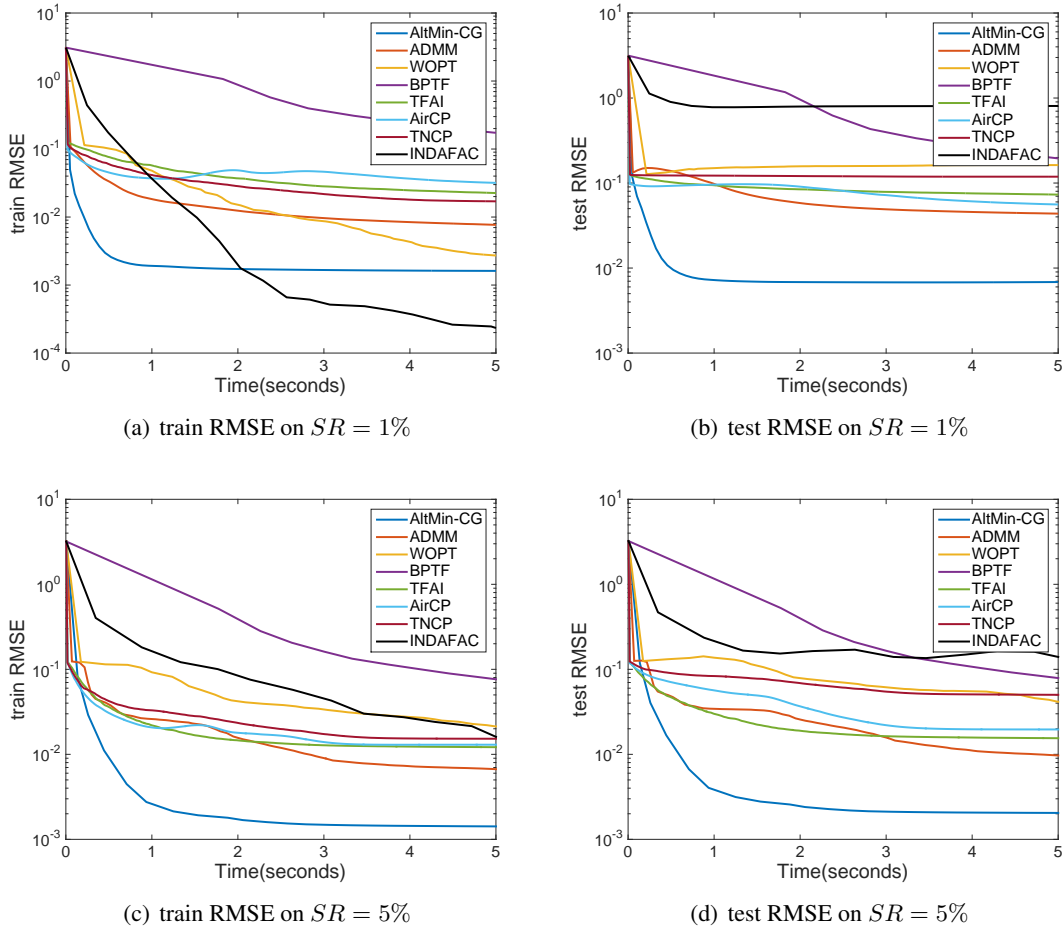


Figure 6. Iterative results of the tested algorithms on the FIA dataset: RMSE on training and test sets by accumulative time per-iteration.

For real data in Figure 5, AirCP, TFAI, AltMin-CG and ADMM have comparable time efficiencies and are the fastest among all tested algorithms in terms of training error. BPTF is slower than the aforementioned methods but obtains the lowest test RMSE. In Figure 6 and Figure 8, we also observe that the proposed AltMin-CG and ADMM methods outperform most other methods both in efficiency and accuracy with the given training data that correspond to low sampling rates.

7. Conclusion. Built on the ideas of a nuclear norm based approach, CP decomposition and graph Laplacian regularizers, we constructed a new low-rank tensor completion model (3.1), also motivated by results in [48] on matrix completion with graph Laplacian. The advantage of the proposed model is twofold: (i) the CP-based decomposition enables a memory-efficient model for low-rank tensors and (ii) the use of the graph Laplacian-based regularizer yields completion results with higher recovery accuracy than several classical, graph-agnostic tensor completion models. An alternating minimization (AltMin) method is proposed. The minimization of each of the subproblems is done by a linear CG routine, in which an efficient Hessian-vector multiplication is used. Besides, the alternat-

ing directions method of multipliers (ADMM) method is also applied to the LRTC model which shows competitive performance. Moreover, the convergence analysis for the proposed AltMin algorithm is given. From the results of various numerical experiments, we verified that the graph-regularized tensor completion model (3.1) produces solutions with better recovery performances compared to graph-agnostic tensor completion models. This observation is especially significant when the sample rate is small. Our proposed algorithms for solving the graph-regularized tensor completion problem, AltMin-CG (Algorithm 4.2) and ADMM (Algorithm 4.5), have been shown to be time efficient compared with other state-of-art methods.

REFERENCES

- [1] E. ACAR, D. M. DUNLAVY, T. G. KOLDA, AND M. MØRUP, *Scalable tensor factorizations for incomplete data*, Chemometrics and Intelligent Laboratory Systems, 106 (2011), pp. 41–56.
- [2] M. V. AFONSO, J. M. BIOUCAS-DIAS, AND M. A. FIGUEIREDO, *An augmented lagrangian approach to the constrained optimization formulation of imaging inverse problems*, IEEE Transactions on Image Processing, 20 (2010), pp. 681–695.
- [3] C. A. ANDERSSON AND R. BRO, *Improving the speed of multi-way algorithms:: Part i. tucker3*, Chemometrics and intelligent laboratory systems, 42 (1998), pp. 93–103.
- [4] H. ATTOUCH, J. BOLTE, P. REDONT, AND A. SOUBEYRAN, *Proximal alternating minimization and projection methods for nonconvex problems: An approach based on the kurdyka-lojasiewicz inequality*, Mathematics of Operations Research, 35 (2010), pp. 438–457.
- [5] B. W. BADER, T. G. KOLDA, ET AL., *Matlab tensor toolbox version 2.5*, Available online, January, 7 (2012).
- [6] J. A. BAZERQUE, G. MATEOS, AND G. B. GIANNAKIS, *Rank regularization and bayesian inference for tensor completion and extrapolation*, IEEE transactions on signal processing, 61 (2013), pp. 5689–5703.
- [7] M. BELKIN AND P. NIYOGI, *Laplacian eigenmaps for dimensionality reduction and data representation*, Neural computation, 15 (2003), pp. 1373–1396.
- [8] J. BENNETT, S. LANNING, ET AL., *The netflix prize*, in Proceedings of KDD cup and workshop, vol. 2007, Citeseer, 2007, p. 35.
- [9] S. BOYD, N. PARIKH, E. CHU, B. PELEATO, J. ECKSTEIN, ET AL., *Distributed optimization and statistical learning via the alternating direction method of multipliers*, Foundations and Trends® in Machine learning, 3 (2011), pp. 1–122.
- [10] R. BRO, *Parafac. tutorial and applications*, Chemometrics and intelligent laboratory systems, 38 (1997), pp. 149–171.
- [11] R. BRO, *Multi-way analysis in the food industry-models, algorithms, and applications*, in MRI, EPG and EMA,” Proc ICSLP 2000, Citeseer, 1998.
- [12] E. J. CANDÈS AND B. RECHT, *Exact matrix completion via convex optimization*, Foundations of Computational mathematics, 9 (2009), p. 717.
- [13] J. CARROLL AND J.-J. CHANG, *Analysis of individual differences in multidimensional scaling via an n-way generalization of Eckart-Young decomposition*, Psychometrika, 35 (1970), pp. 283–319, <http://dx.doi.org/10.1007/BF02310791>. 10.1007/BF02310791.
- [14] B. CHAZELLE, *An improved algorithm for the fixed-radius neighbor problem*, Information Processing Letters, 16 (1983), pp. 193–198.
- [15] J. CHEN, H. A. GOV, AND Y. SAAD, *Fast Approximate kNN Graph Construction for High Dimensional Data via Recursive Lanczos Bisection Haw-ren Fang*, Journal of Machine Learning Research, 10 (2009), <http://www.jmlr.org/papers/volume10/chen09b/chen09b.pdf>.
- [16] W. CHU AND Z. GHAMRANI, *Probabilistic models for incomplete multi-dimensional arrays*, in Artificial Intelligence and Statistics, 2009, pp. 89–96.
- [17] F. R. CHUNG AND F. C. GRAHAM, *Spectral graph theory*, no. 92, American Mathematical Soc., 1997.
- [18] C. DA SILVA AND F. HERRMANN, *Hierarchical tucker tensor optimization-applications to tensor completion. sampta 2013*, in 10th International Conference on Sampling Theory and Application, Jacobs University Bremen, 2013.
- [19] L. DE LATHAUWER, B. DE MOOR, AND J. VANDEWALLE, *A multilinear singular value decomposition*, SIAM J.

- Matrix Anal. Appl., 21 (2000), pp. 1253–1278 (electronic), <https://doi.org/10.1137/S0895479896305696>, <http://dx.doi.org/10.1137/S0895479896305696>.
- [20] L. DE LATHAUWER, B. DE MOOR, AND J. VANDEWALLE, *On the best rank-1 and rank- (R_1, R_2, \dots, R_N) approximation of higher-order tensors*, SIAM J. Matrix Anal. Appl., 21 (2000), pp. 1324–1342 (electronic), <https://doi.org/10.1137/S0895479898346995>, <http://dx.doi.org/10.1137/S0895479898346995>.
- [21] S. DONG, P.-A. ABSIL, AND K. A. GALLIVAN, *Riemannian gradient descent methods for graph-regularized matrix completion*, Preprint, (2019), pp. 1–41, <https://sites.uclouvain.be/absil/2019.06>.
- [22] N. K. M. FABER, R. BRO, AND P. K. HOPKE, *Recent developments in candecomp/parafac algorithms: a critical review*, Chemometrics and Intelligent Laboratory Systems, 65 (2003), pp. 119 – 137, [https://doi.org/10.1016/S0169-7439\(02\)00089-8](https://doi.org/10.1016/S0169-7439(02)00089-8), <http://www.sciencedirect.com/science/article/pii/S0169743902000898>.
- [23] M. FAZEL, H. HINDI, S. P. BOYD, ET AL., *A rank minimization heuristic with application to minimum order system approximation*, in Proceedings of the American control conference, vol. 6, Citeseer, 2001, pp. 4734–4739.
- [24] S. GANDY, B. RECHT, AND I. YAMADA, *Tensor completion and low-n-rank tensor recovery via convex optimization*, Inverse Problems, 27 (2011), p. 025010.
- [25] H. GE, J. CAVERLEE, N. ZHANG, AND A. SQUICCIARINI, *Uncovering the spatio-temporal dynamics of memes in the presence of incomplete information*, in Proceedings of the 25th ACM International on Conference on Information and Knowledge Management, ACM, 2016, pp. 1493–1502.
- [26] H. GE, K. ZHANG, M. ALFIFI, X. HU, AND J. CAVERLEE, *Distenc: A distributed algorithm for scalable tensor completion on spark*, in 2018 IEEE 34th International Conference on Data Engineering (ICDE), IEEE, 2018, pp. 137–148.
- [27] T. GOLDSTEIN AND S. OSHER, *The split bregman method for l_1 -regularized problems*, SIAM journal on imaging sciences, 2 (2009), pp. 323–343.
- [28] R. HARSHMAN, *Foundations of the parafac procedure: Models and conditions for an "explanatory" multi-modal factor analysis*, UCLA Working Papers in Phonetics, 16 (1970).
- [29] X. HE AND P. NIYOGI, *Locality preserving projections*, in Advances in neural information processing systems, 2004, pp. 153–160.
- [30] F. HITCHCOCK, *The Expression of a Tensor Or a Polyadic as a Sum of Products*, Contributions from the Department of Mathematics, sn., 1927, <http://books.google.com/books?id=G7VOHAAACAAJ>.
- [31] A. KARATZOGLOU, X. AMATRIAIN, L. BALTRUNAS, AND N. OLIVER, *Multiverse recommendation: n-dimensional tensor factorization for context-aware collaborative filtering*, in Proceedings of the fourth ACM conference on Recommender systems, ACM, 2010, pp. 79–86.
- [32] H. A. KIERS, J. M. TEN BERGE, AND R. BRO, *Parafac2—part i. a direct fitting algorithm for the parafac2 model*, Journal of Chemometrics: A Journal of the Chemometrics Society, 13 (1999), pp. 275–294.
- [33] H. A. L. KIERS, *Towards a standardized notation and terminology in multiway analysis*, Journal of Chemometrics, 14 (2000), pp. 105–122, [https://doi.org/10.1002/1099-128X\(200005/06\)14:3<105::AID-CEM582>3.0.CO;2-I](https://doi.org/10.1002/1099-128X(200005/06)14:3<105::AID-CEM582>3.0.CO;2-I), [http://dx.doi.org/10.1002/1099-128X\(200005/06\)14:3<105::AID-CEM582>3.0.CO;2-I](http://dx.doi.org/10.1002/1099-128X(200005/06)14:3<105::AID-CEM582>3.0.CO;2-I).
- [34] S. G. KRANTZ AND H. R. PARKS, *A primer of real analytic functions*, Springer Science & Business Media, 2002.
- [35] P. M. KROONENBERG, *Three-mode principal component analysis: Theory and applications*, vol. 2, DSWO press, 1983.
- [36] H. LAMBA, V. NAGARAJAN, K. SHIN, AND N. SHAJARISALES, *Incorporating side information in tensor completion*, in Proceedings of the 25th International Conference Companion on World Wide Web, International World Wide Web Conferences Steering Committee, 2016, pp. 65–66.
- [37] Y. LI, J. YAN, Y. ZHOU, AND J. YANG, *Optimum subspace learning and error correction for tensors*, in European Conference on Computer Vision, Springer, 2010, pp. 790–803.
- [38] A. P. LIAVAS AND N. D. SIDIROPOULOS, *Parallel algorithms for constrained tensor factorization via alternating direction method of multipliers*, IEEE Transactions on Signal Processing, 63 (2015), pp. 5450–5463.
- [39] J. LIU, P. MUSIALSKI, P. WONKA, AND J. YE, *Tensor completion for estimating missing values in visual data*, in 2009 IEEE 12th International Conference on Computer Vision, IEEE, 2009, pp. 2114–2121.
- [40] J. LIU, P. MUSIALSKI, P. WONKA, AND J. YE, *Tensor completion for estimating missing values in visual data*, IEEE transactions on pattern analysis and machine intelligence, 35 (2012), pp. 208–220.
- [41] Y. LIU, F. SHANG, L. JIAO, J. CHENG, AND H. CHENG, *Trace norm regularized candecomp/parafac decomposition with missing data*, IEEE transactions on cybernetics, 45 (2014), pp. 2437–2448.
- [42] R. MAZUMDER, T. HASTIE, H. EDU, R. TIBSHIRANI, T. EDU, AND T. JAakkola, *Spectral Regularization Algorithms for Learning Large Incomplete Matrices*, Journal of Machine Learning Research, 11 (2010), pp. 2287–

- 2322, <https://web.stanford.edu/~hastie/Papers/mazumder10a.pdf>.
- [43] B. S. MORDUKHOVICH, *Variational analysis and generalized differentiation I: Basic theory*, vol. 330, Springer Science & Business Media, 2006.
- [44] A. NARITA, K. HAYASHI, R. TOMIOKA, AND H. KASHIMA, *Tensor factorization using auxiliary information*, *Data Mining and Knowledge Discovery*, 25 (2012), pp. 298–324.
- [45] E. E. PAPALEXAKIS, C. FALOUTSOS, AND N. D. SIDIROPOULOS, *Tensors for data mining and data fusion: Models, applications, and scalable algorithms*, *ACM Transactions on Intelligent Systems and Technology (TIST)*, 8 (2017), p. 16.
- [46] N. PERRAUDIN, J. PARATTE, D. SHUMAN, L. MARTIN, V. KALOFOLIAS, P. VANDERGHEYNST, AND D. K. HAMMOND, *Gspbox: A toolbox for signal processing on graphs*, arXiv preprint arXiv:1408.5781, (2014).
- [47] N. RAO, H.-F. YU, P. RAVIKUMAR, AND I. S. DHILLON, *Collaborative Filtering with Graph Information: Consistency and Scalable Methods*, in *Advances in Neural Information Processing Systems* 28, 2015, pp. 2107–2115, <http://papers.nips.cc/paper/5938-collaborative-filtering-with-graph-information-consistency-and-scalable-methods.pdf>.
- [48] N. RAO, H.-F. YU, P. K. RAVIKUMAR, AND I. S. DHILLON, *Collaborative filtering with graph information: Consistency and scalable methods*, in *Advances in neural information processing systems*, 2015, pp. 2107–2115.
- [49] H. RAUHUT, R. SCHNEIDER, AND Ž. STOJANAC, *Tensor completion in hierarchical tensor representations*, in *Compressed Sensing and its Applications*, Springer, 2015, pp. 419–450.
- [50] H. RAUHUT, R. SCHNEIDER, AND Ž. STOJANAC, *Low rank tensor recovery via iterative hard thresholding*, *Linear Algebra and its Applications*, 523 (2017), pp. 220–262.
- [51] B. RECHT, M. FAZEL, AND P. A. PARRILO, *Guaranteed minimum-rank solutions of linear matrix equations via nuclear norm minimization*, *SIAM review*, 52 (2010), pp. 471–501.
- [52] R. T. ROCKAFELLAR AND R. J.-B. WETS, *Variational analysis*, vol. 317, Springer Science & Business Media, 2009.
- [53] Z. SHI, J. HAN, T. ZHENG, AND J. LI, *Guarantees of augmented trace norm models in tensor recovery*, in *Twenty-Third International Joint Conference on Artificial Intelligence*, 2013.
- [54] N. SREBRO, J. RENNIE, AND T. S. JAAKKOLA, *Maximum-margin matrix factorization*, in *Advances in neural information processing systems*, 2005, pp. 1329–1336.
- [55] N. SREBRO AND A. SHRAIBMAN, *Rank, trace-norm and max-norm*, in *International Conference on Computational Learning Theory*, Springer, 2005, pp. 545–560.
- [56] G. TOMASI AND R. BRO, *Parafac and missing values*, *Chemometrics and Intelligent Laboratory Systems*, 75 (2005), pp. 163–180.
- [57] L. TUCKER, *Some mathematical notes on three-mode factor analysis*, *Psychometrika*, 31 (1966), pp. 279–311, <http://dx.doi.org/10.1007/BF02289464>.
- [58] L. XIONG, X. CHEN, T.-K. HUANG, J. SCHNEIDER, AND J. G. CARBONELL, *Temporal collaborative filtering with bayesian probabilistic tensor factorization*, in *Proceedings of the 2010 SIAM international conference on data mining*, SIAM, 2010, pp. 211–222.
- [59] Y. XU AND W. YIN, *A block coordinate descent method for regularized multiconvex optimization with applications to nonnegative tensor factorization and completion*, *SIAM Journal on imaging sciences*, 6 (2013), pp. 1758–1789.
- [60] L. YANG, Z.-H. HUANG, AND X. SHI, *A fixed point iterative method for low n-rank tensor pursuit*, *IEEE Transactions on Signal Processing*, 61 (2013), pp. 2952–2962.
- [61] Q. ZHAO, L. ZHANG, AND A. CICHOCKI, *Bayesian cp factorization of incomplete tensors with automatic rank determination*, *IEEE transactions on pattern analysis and machine intelligence*, 37 (2015), pp. 1751–1763.
- [62] Q. ZHAO, L. ZHANG, AND A. CICHOCKI, *Bayesian sparse tucker models for dimension reduction and tensor completion*, arXiv preprint arXiv:1505.02343, (2015).

Supplementary Material

Appendix A. Supplementary results in the experiments.

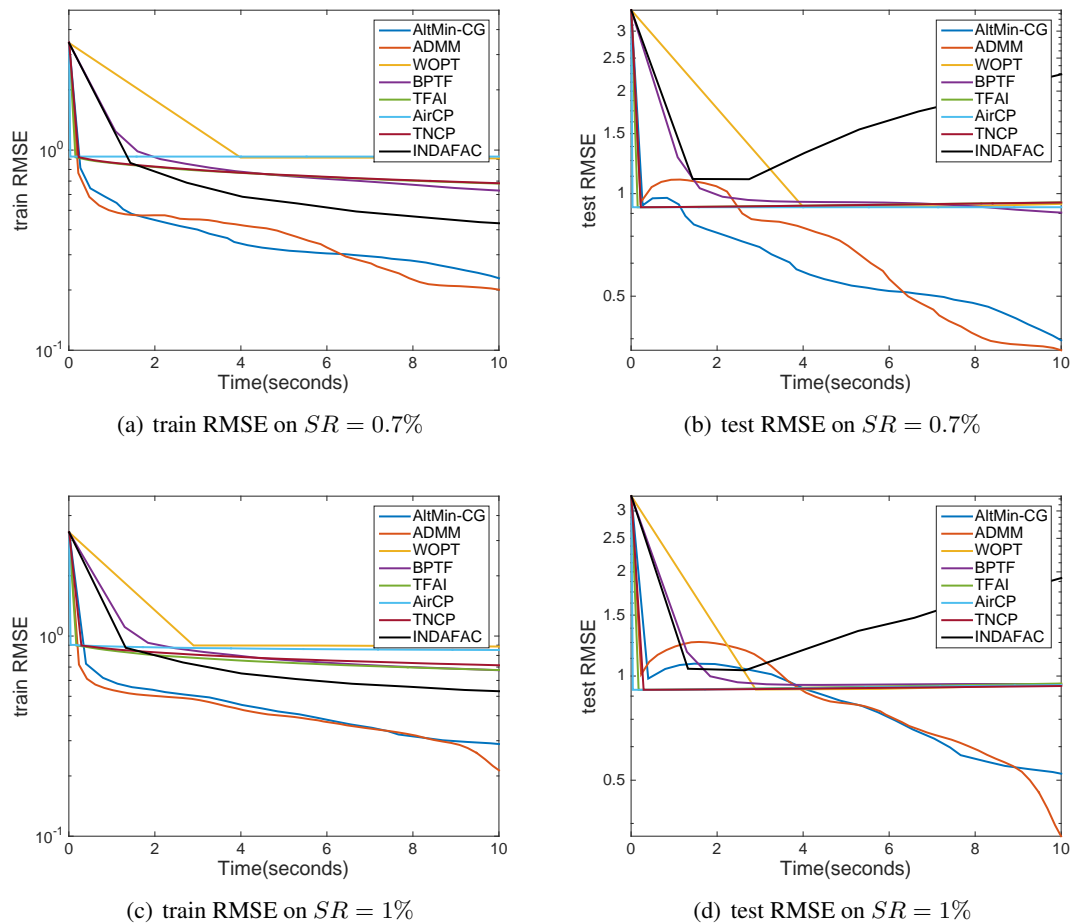


Figure 7. Iterative results of the tested algorithms on synthetic data: RMSE on training and test sets by accumulative time per-iteration. The sampling rates tested are 0.7% and 1%.

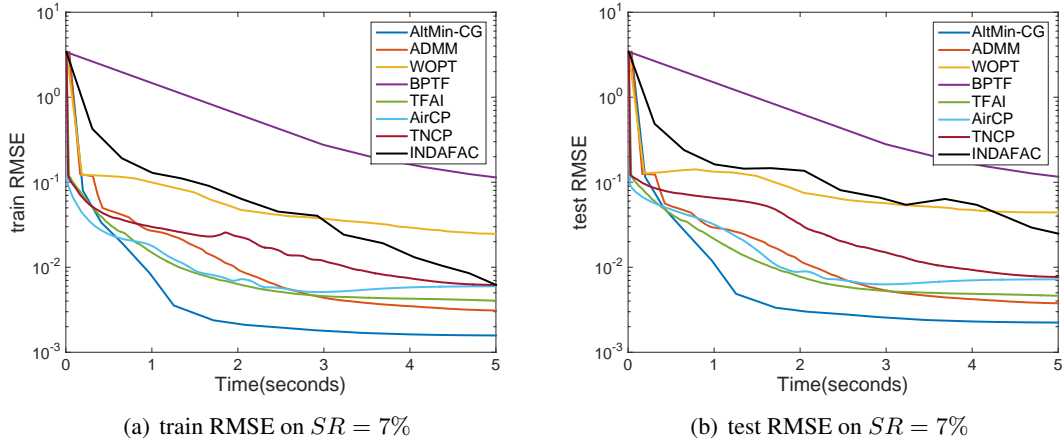


Figure 8. Iterative results of the tested algorithms on the FIA dataset: RMSE on training and test sets by accumulative time per-iteration.

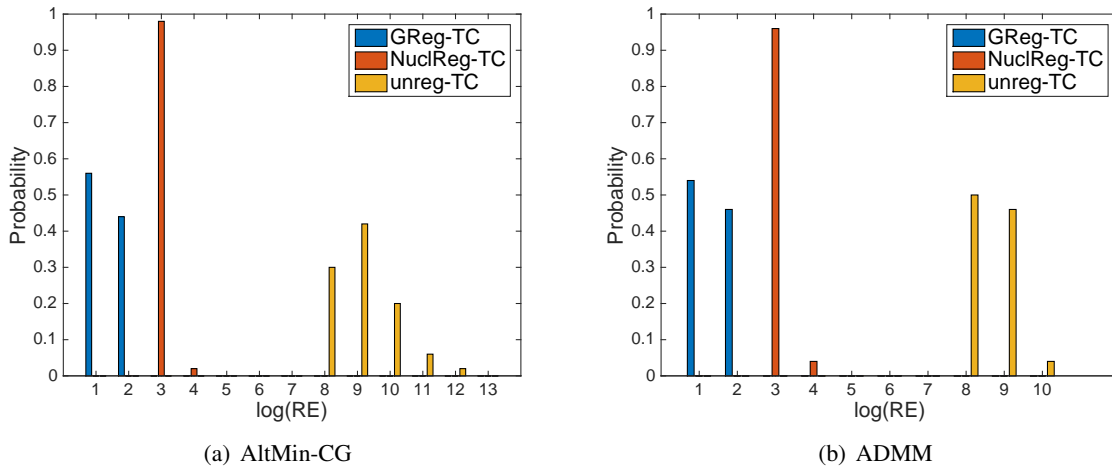


Figure 9. Recovery accuracies (relative error) of the three models on synthetic data. The sampling rate $SR = 0.5\%$.

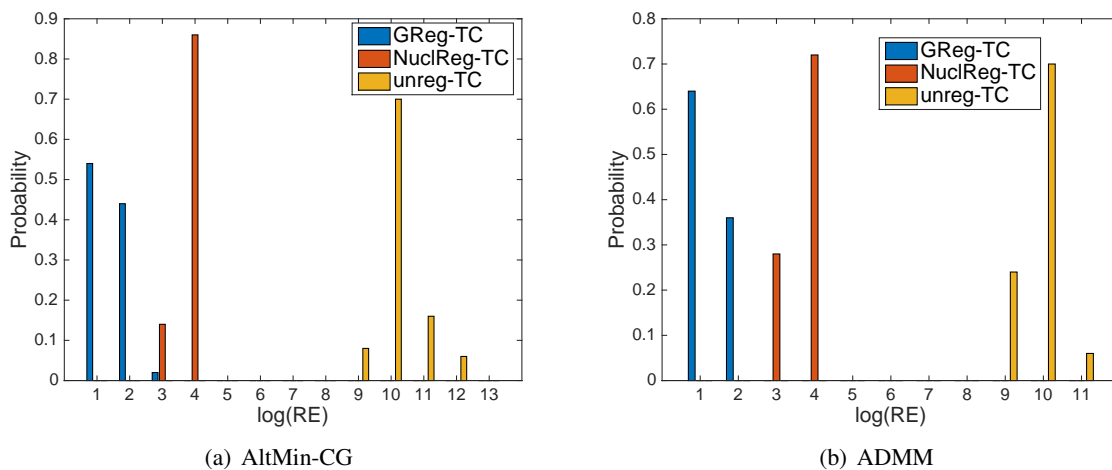


Figure 10. Recovery accuracies (relative error) of the three models on synthetic data. The sampling rate $SR = 0.7\%$.

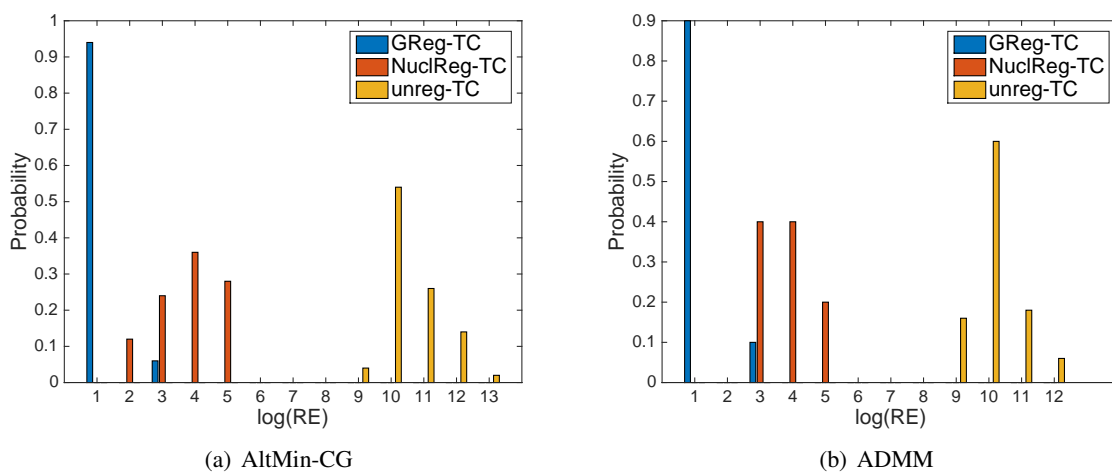


Figure 11. Recovery accuracies (relative error) of the three models on synthetic data. The sampling rate $SR = 1\%$.

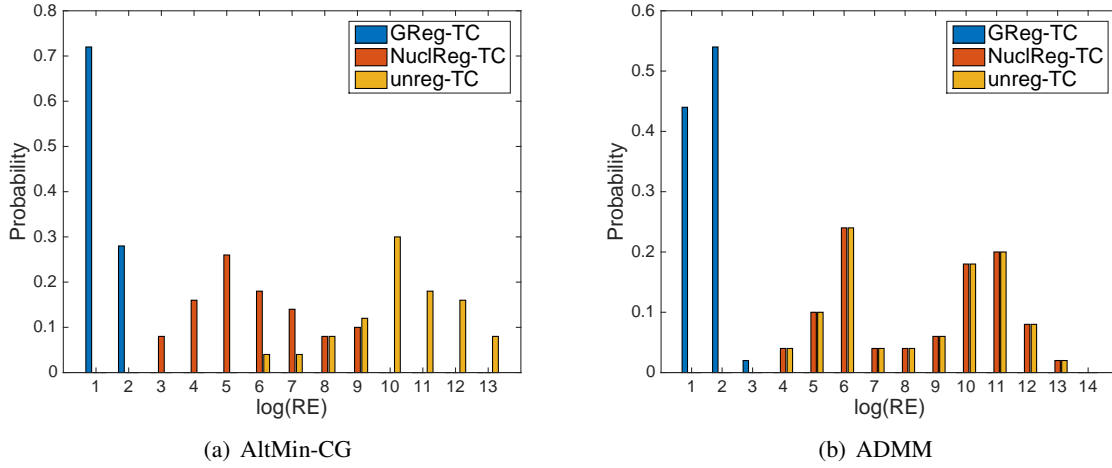


Figure 12. Recovery accuracies (relative error) of the three models on synthetic data. The sampling rate $SR = 5\%$.

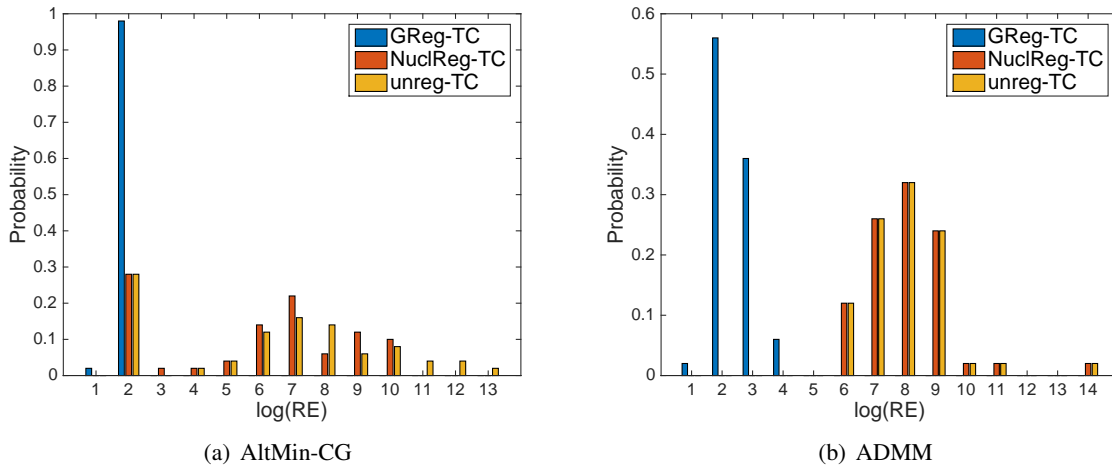


Figure 13. Recovery accuracies (relative error) of the three models on synthetic data. The sampling rate $SR = 7\%$.

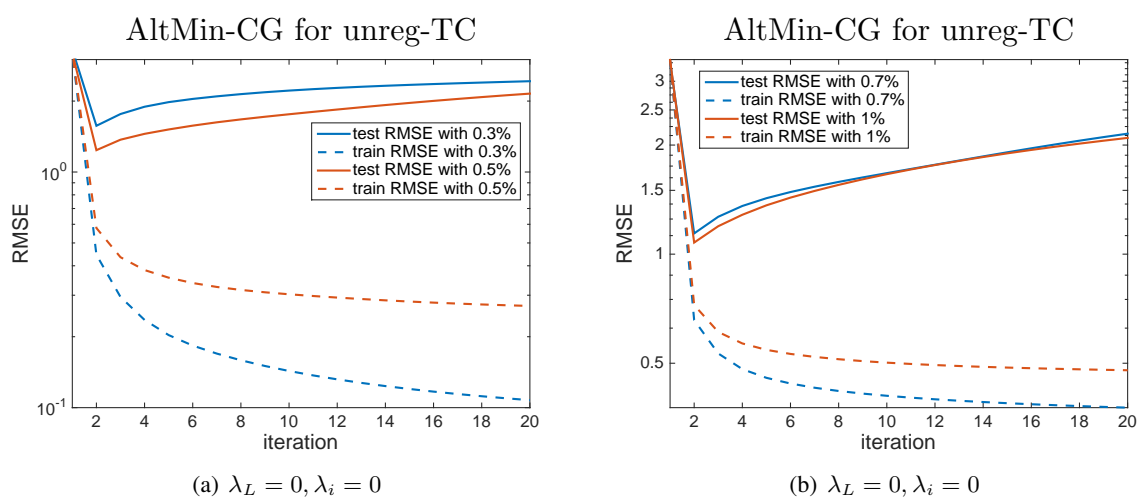


Figure 14. Iterative results of the unregularized model: RMSE on training and test sets per iteration. The sampling rates are too low for the unregularized model to generalize the completion result on the training set to the test set.